Cross Sections and Related Data for Electron Collisions with Hydrogen Molecules and Molecular Ions[a)]

H. Tawara, Y. Itikawa,[b)] H. Nishimura,[c)] and M. Yoshino[d)]

National Institute for Fusion Science,[e)] Nagoya 464-01, Japan

(Received July 5, 1989; revised manuscript received November 1, 1989)

Data are compiled and evaluated for collision processes of excitation, dissociation, ionization, attachment, and recombination of hydrogen molecules and molecular ions (H_2^+, H_3^+) by electron impact as well as for properties of their collision products.

Key words: electron impact; hydrogen molecule; hydrogen molecular ion; scattering; elastic integral; vibrational excitation; rotational excitation; dissociation; ionization; photon emission; cross section.

Contents

1. Introduction 618
2. Cross Sections for Various Collision Processes.... 618
   2.1. Total and Elastic Scattering 618
   2.2. Excitation of H_2 molecules 620
      2.2.1. Rotational Excitation 620
      2.2.2. Vibrational Excitation 620
      2.2.3. Electronic Excitation 622
   2.3. Dissociative Excitation of H_2 Molecules... 622
      2.3.1. Emission Cross Sections of Balmer-α, -β, -γ, and -δ Lines from H_2 623
      2.3.2. Emission Cross Sections of Lyman-α and -β Lines from H_2 625
      2.3.3. Cross Sections for the Production of Metastable H(2s) State Atoms from H_2 Molecules 625
      2.3.4. Cross Sections for Dissociative Excitation of H_2 to High Rydberg States . 626
      2.3.5. Emission Cross Sections of the Werner- and Lyman-band Systems of H_2 626
   2.4. Ionization and Dissociative Ionization of H_2 626
   2.5 Dissociative Attachment to H_2 627
   2.6 Collisions of H_2^+ Ions 627
   2.7 Collisions of H_3^+ Ions 629
3. Characteristics of Products from H_2..... 630
   3.1. Hydrogen Atoms from Dissociative Excitation/Ionization of H_2 630
      3.1.1. Hydrogen Atoms in the Ground State 630
      3.1.2. Hydrogen Atoms in the Excited States 630
   3.2. Protons from Dissociative Ionization of H_2 631
   3.3. Protons from Double Ionization of H_2 634
4. Concluding Remarks and Comments on Future Work 635
5. Acknowledgment 635
6. References 635

List of Figures

1. Some important energy levels of molecular hydrogen and molecular ion. 619
2. Comparison of cross sections for various collision processes in neutral H_2 620
3. Cross sections of elastic scattering. 621
4. Cross sections of rotational excitation. 621
5. Cross sections of vibrational excitation. 622
6. Cross sections of electronic excitation to $B\,^1\Sigma_u^+$.. 623
7. Cross sections of electronic excitation to B' and $B''\,^1\Sigma_u^+$. 623
8. Cross sections of electronic excitation to $C\,^1\Pi_u$... 623
9. Cross sections of electronic excitation to D and $D'\,^1\Pi_u$. 623
10. Cross sections of electronic excitation to $E\,^1\Sigma_g^+$. 623
11. Cross sections of electronic excitation to $a\,^3\Sigma_g^+$. 624
12. Cross sections of electronic excitation to $b\,^3\Sigma_u^+$. 624
13. Cross sections of electronic excitation to $c\,^3\Pi_u$.. 624
14. Cross sections of electronic excitation to $e\,^3\Sigma_u^+$. 624
15. Cross sections of photon emission for Lyman band, Werner band, Lyman-α, Lyman-β, 2s state, Balmer-α, -β, -γ, and -δ lines. 625

[a)] Preliminary results of the present report have been described in IPPJ-AM-46 (1986) and IPPJ-AM-55 (1987, Institute of Plasma Physics, Nagoya University, Nagoya 464-01, Japan)

[b)] Institute of Space and Astronautical Science, Sagamihara 229, Japan
[c)] Physics Department, Niigata University, Niigata 950-21, Japan
[d)] General College of Education, Shibaura Institute of Technology, Ohmiya 330, Japan
[e)] Formerly Institute of Plasma Physcis, Nagoya University

© 1990 by the U. S. Secretary of Commerce on behalf of the United States. This copyright is assigned to the American Institute of Physics and the American Chemical Society.
Reprints available from ACS; see Reprints List at back of issue.

Downloaded 24 Jun 2013 to 128.112.200.107. This article is copyrighted as indicated in the abstract. Reuse of AIP content is subject to the terms at: http://jpcrd.aip.org/about/rights_and_permissions

16. Cross sections of the production for total ion, molecular hydrogen ions, protons and double protons. 626
17. Cross sections of dissociative attachment for HD and D_2 as well as H_2. 627
18. Cross sections of electron collisions with $H(v)_2^+$ ions for the production of atomic hydrogen. 628
19. Cross sections of electron collisions with H_3^+ ions for the production of total atomic hydrogens (rf ion source and trap ion source), total protons and $H_2^+ + H^-$. 629
20. Doppler-shifted spectral shapes of Balmer-β line as a function of the electron impact energy. 631
21. Potential energy curves of H_2, H_2^+ and H_2^{2+} and the expected energy distributions of protons produced via $^2\Sigma_g^+$ and $^2\Sigma_u^+$ states of H_2^+ in dissociative ionization of H_2. 632
22. Ratios of H^+/H_2^+ in electron impact. 632
23. Cross sections of production of protons with the energy above 0.25 eV and their fractions. 632
24. Proton energy spectra at different electron impact energies. 633
25. Relative angular distributions of 8.6 eV protons produced from H_2 in various electron impact energies. 633
26. Angular anisotropy of protons with the energy of 3, 4, 5, 6, and 7 eV at the electron impact energy of 40 eV. 634
27. Energy distribution of protons from doubly ionized hydrogen molecules in electron impact. 634

1. INTRODUCTION

A number of experimental and theoretical investigations of collision processes involving hydrogen molecules and molecular ions in electron impact have been and are still being performed extensively because they are of the most fundamental importance in electron-molecule collisions. Indeed, understanding of electron-molecule collision processes is requisite in many applications such as chemistry, astrophysics, astrochemistry, plasma fusion research, and plasma material processing. Thus, there are a number of review articles on hydrogen molecule and molecular ion collisions with electrons available presently.[1–4] The cross sections for various collision processes such as excitation, dissociation, ionization or photon emission have to be known with appropriate accuracies for such applications, modelling and diagnostics. Also various features, such as energy distributions and angular (spatial) distributions, of products, either ions, atoms, molecules or photons, are key parameters necessary in understanding electron-molecule or electron-molecular-ion collisions and also in modelling of molecule-related phenomena such as plasma behavior. For example, the energy distributions of atomic hydrogens produced through dissociative processes are decisive in determining the mean free path for ionization in media such as plasmas. As will be seen later, these data with high accuracies are still limited. Only very few compilation of such data are available presently.

Some experimental data, though taken in relatively early days, seem to be reliable and are included in the present compilation and evaluation. If the absolute values seem not to be certain but to show reasonable (asymptotic) energy dependence, then, they are renormalized to some, recently well established or accurate values to get the final cross sections over a wide range of the collision energy. In particular, as the measured cross sections of photon emission (see Sec. 2.3. in particular) are strongly dependent upon the accuracies of calibration methods of detector sensitivities, reliable light sources are requisite. Indeed new continuous light sources (for example, synchrotron radiation source) with the known intensities over a wide range of photon energy have recently become available and the accuracies in related excitation cross-section data, for example, through photon observations, are expected to be improved significantly.

Some serious discrepancies have often been observed in the cross sections for dissociation or ionization products or their angular distributions or energy distributions because their collection efficiencies could be hard to estimate accurately or unreliable or even unknown as the products have their, relatively large, initial kinetic energies.

New theoretical calculations, based upon newly developed techniques or new approximations, are generally more accurate than old values and, then, are included.

We show in Fig. 1 some of the important potential energy curves of hydrogen molecules H_2 and molecular ions H_2^+ taken from a paper by Sharp.[5]

2. Cross Sections for Various Collision Processes

In the present work, the evaluation of cross-section data for various collision processes is based mostly upon experimental results as far as they are available. Many of the theoretical results seem still uncertain because of inherent complexity of molecular calculations, though some sophisticated calculations reproduce the observed results quite well. For comparison, the calculated values are also shown with experimental data in the following figures. Some experimental data are excluded because they might include the contribution of other processes due to the limited resolution of experimental systems.

The cross sections evaluated for various excitation processes as well as the total cross sections and inelastic cross sections are shown and their magnitudes are compared in Fig. 2. These numerical data are available upon request.

2.1. Total and Elastic Scattering

Total cross sections are taken from those recommended by Hayashi,[6] meanwhile integral elastic and other cross sections are based upon the present evaluation (see Fig. 2).

Integral elastic cross sections were determined by a number of workers through measuring the attenuation of

Downloaded 24 Jun 2013 to 128.112.200.107. This article is copyrighted as indicated in the abstract. Reuse of AIP content is subject to the terms at: http://jpcrd.aip.org/about/rights_and_permissions

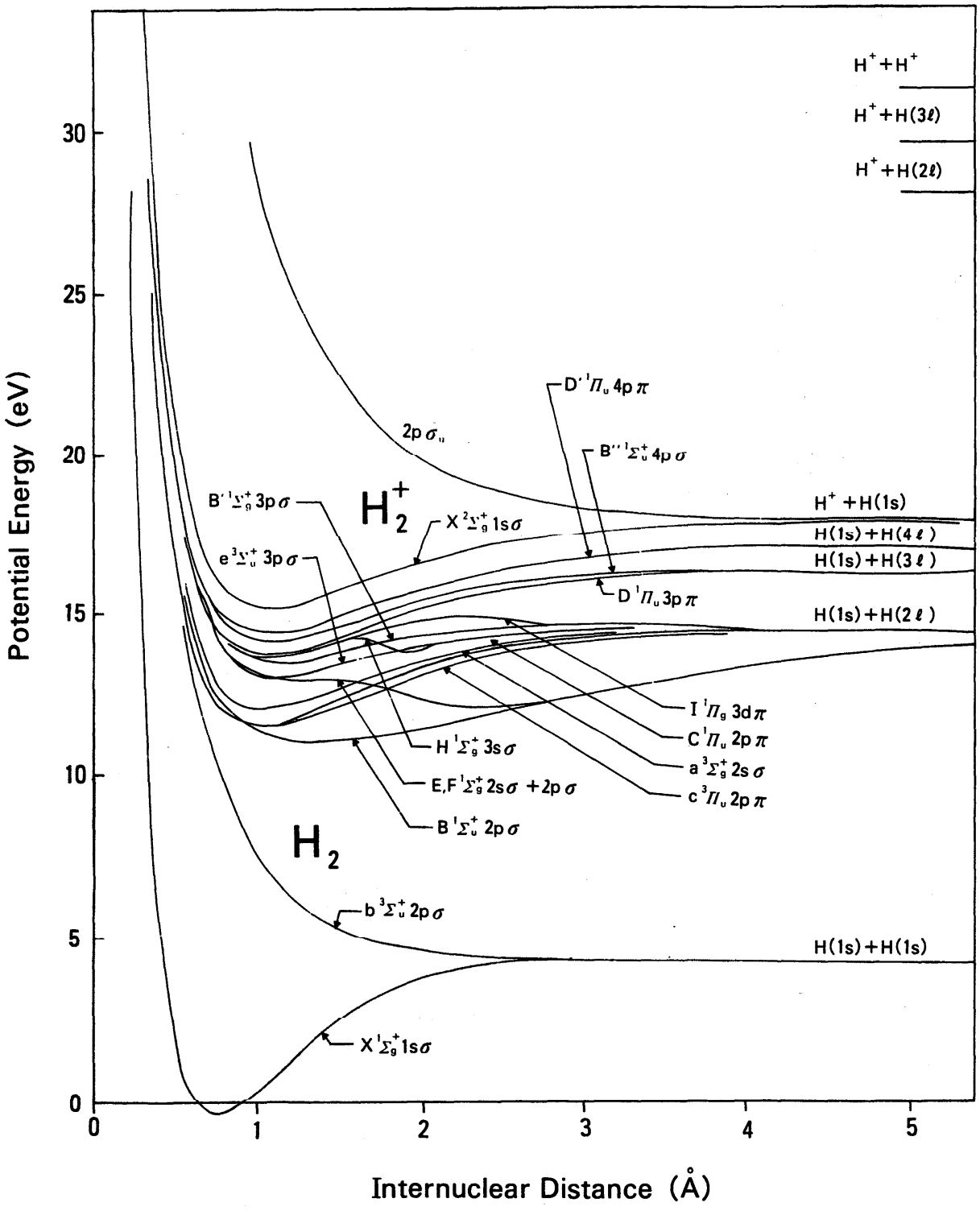


FIG. 1. Some important energy levels of molecular hydrogen and molecular ion (see Ref. 5).

Downloaded 24 Jun 2013 to 128.112.200.107. This article is copyrighted as indicated in the abstract. Reuse of AIP content is subject to the terms at: http://jpcrd.aip.org/about/rights and permissions

electron beam intensities or integrating differential scattering cross sections and, thus, indicate the sum of elastic cross sections and rotational excitation cross sections. Those by van Wingerden *et al.*,[7] Shyn and Sharp,[8] and Nishimura *et al.*[9] are shown in Fig. 3. The detailed comparison among other cross-section data[10] on elastic scattering has recently been given by Nishimura *et al.*[9]

2.2 Excitation of H_2

Excitation processes have been usually studied with swarm method, electron energy-loss spectroscopy or photon spectroscopy. In Table 1 are summarized experimental and theoretical studies where the cross sections have been determined or calculated.

2.2.1. Rotational Excitation

The following processes have been investigated experimentally:

$$e + H_2(X\,^1\Sigma_g, v = 0, J = 0) \rightarrow e + H_2(X\,^1\Sigma_g, v = 0, J = 2), \quad (2\text{-}1)$$

$$e + H_2(X\,^1\Sigma_g, v = 0, J = 1) \rightarrow e + H_2(X\,^1\Sigma_g, v = 0, J = 3). \quad (2\text{-}2)$$

Rotational excitation cross sections measured by Crompton *et al.*[11] ($J = 0 \rightarrow 2$: swarm), Gibson[12] ($J = 1 \rightarrow 3$: swarm) and Linder and Schmidt[13] ($J = 1 \rightarrow 3$: beam) are shown in Fig. 4. At low energies, the isotope effects are clearly seen between H_2 and D_2.

2.2.2. Vibrational Excitation

A number of measurements for vibrational excitation cross sections have been reported:

$$e + H_2(X\,^1\Sigma_g, v = 0) \rightarrow e + H_2(X\,^1\Sigma_g, v = 1,2,3,4,5,6). \quad (2\text{-}3)$$

Most of the measurements were carried out with rotational states unresolved. The cross sections of vibrational excita-

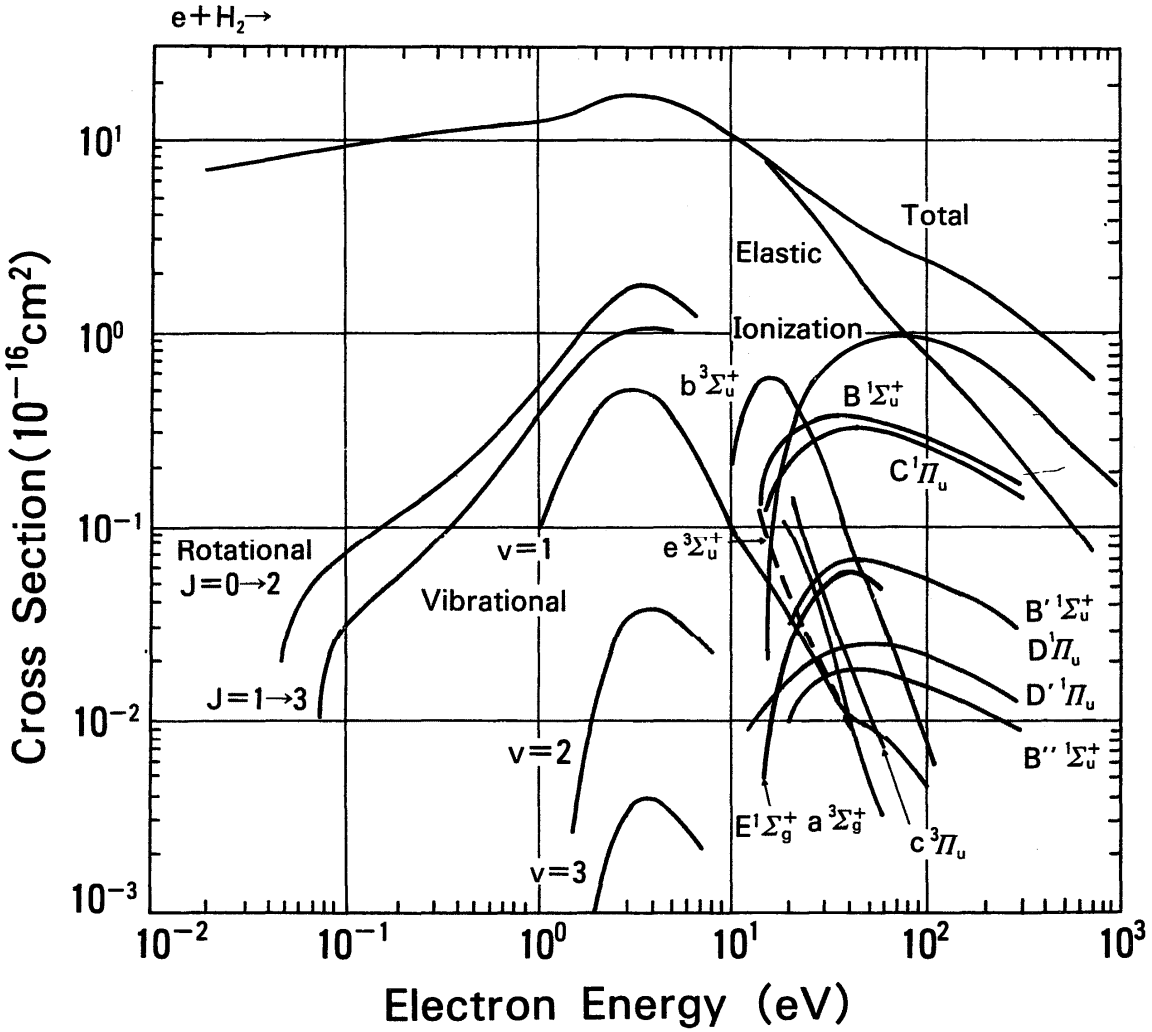


FIG. 2. Comparison of cross sections for various collision processes in neutral H_2. Also for comparison, cross sections of ionization of atomic hydrogen are shown. These data are taken at room temperatures.

Downloaded 24 Jun 2013 to 128.112.200.107. This article is copyrighted as indicated in the abstract. Reuse of AIP content is subject to the terms at: http://jpcrd.aip.org/about/rights_and_permissions

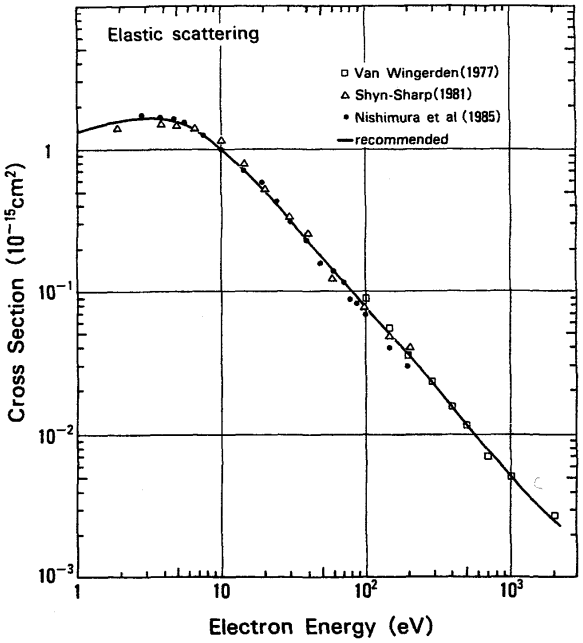


FIG. 3. Cross sections of elastic scattering.

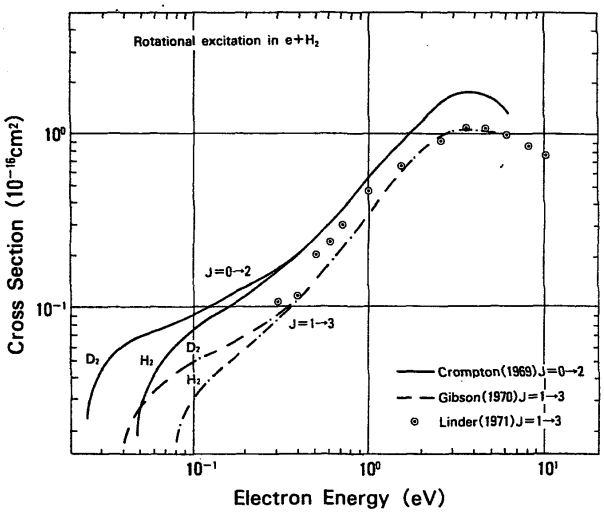


FIG. 4. Cross sections of rotational excitation.

tion with rotational states resolved were determined by Linder and Schmidt[13] ($v=0\rightarrow1$, $\Delta J=0$, and $J=1\rightarrow3$:beam). The cross sections for higher vibrational states were reported by Ehrhardt *et al.*[15] ($v=1,2,3$:beam). Allan[16] ($v=1,2,3,4,5,6$:beam) obtained relative cross sections for various vibrational states and normalized them to the value of Ehrhardt *et al.*[15] for $v=1$ state.

Also theoretical calculations were reported for various vibrational excitation in low-energy region (below 10 eV). Extensive discussion on theoretical aspects has been given by Lane.[24] The most complete calculation of the cross sections for vibrational excitation reported so far has been made by Klonover and Kaldor[25] who treated *ab initio* the static, electron-exchange and polarization interactions but resorted the adiabatic nuclei approximation. The adiabatic nuclei approximation has been examined by Morrison *et al.*[26] who found that the agreement was satisfactory except in the near-threshold region (below 2 eV). More recently, Morrison *et al.*[27] have made a detailed calculation of the vibrational cross sections for the electron energies below 10 eV and found a significant discrepancy between their calculation and swarm experiment.[11] To reconcile this discrepancy, they also reana-

TABLE 1. A list of experimental and theoretical work on rotational, vibrational, and electronic excitation processes.

Excited state	References: Experiment	References: Theory
$X\ ^1\Sigma_g^+, v=0, J=0\rightarrow2$	11	
$J=1\rightarrow3$	12,13	
$v=0\rightarrow1$ (J:unresolved)	9,11,14,15,16	25
($\Delta J=0$ and $J=1\rightarrow3$)	13	
$B\ ^1\Sigma_u^+$	17,18,19	30,31,34,36,37,39,45
$B'\ ^1\Sigma_u^+$		30,31,40,45
$B''\ ^1\Sigma_u^+$	17,18	30,31
$C\ ^1\Pi_u$	17,18,19,20	30,31,40
$D\ ^1\Pi_u$		30,31
$D'\ ^1\Pi_u$	17,18	30,31
$E\ ^1\Sigma_g^+$		30,31,39,40
$F\ ^1\Sigma_g^+$		30,31,39,40
$H\ ^1\Sigma_g^+$		30,31
$I\ ^1\Pi_g$		30,31
$a\ ^3\Sigma_g^+$	9	32,34,42,48
$b\ ^3\Sigma_u^+$	21,22,23	32,33,34,36,38,41, 42,43,44,46,47,48,102
$c\ ^3\Pi_u$	19	32,34,40,48
$e\ ^3\Sigma_u^+$		32,34

Downloaded 24 Jun 2013 to 128.112.200.107. This article is copyrighted as indicated in the abstract. Reuse of AIP content is subject to the terms at: http://jpcrd.aip.org/about/rights_and_permissions

lyzed the previous swarm result. The disagreement, however, could not be removed and still remains a problem. For the energies higher than 10 eV, relatively few calculations have been performed. Lee and Freitas[28] applied their incoherent renormalized multicenter potential model to the vibrational excitation, in which they took into account approximately the electron-exchange and polarization effects. They gave only differential cross sections. However, there is a large discrepancy depending upon the scattering angles, though an overall agreement is observed with the measured data. Furthermore, Truhlar *et al.*[29] made the Born and modified Born calculations up to 912 eV but their values are much dependent upon the effective potential adopted in their calculation. The cross sections for vibrational excitation are summarized in Fig. 5, together with theoretical calculation for the excitation $v = 0 \rightarrow 1$ by Klonover and Kaldor.[25]

2.2.3. Electronic Excitation

The following electronic excitation processes have been studied either experimentally or theoretically:

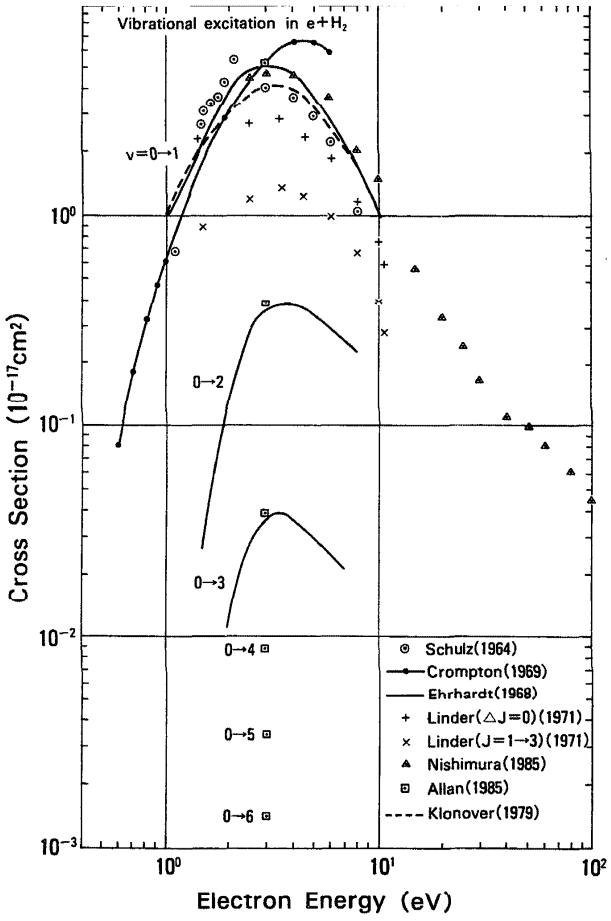


FIG. 5. Cross sections of vibrational excitation.

$$e + H_2(X\,^1\Sigma_g^+) \rightarrow e + H_2(B\,^1\Sigma_u^+) \quad (2\text{-}4)$$

$$(B'\,^1\Sigma_u^+) \quad (2\text{-}5)$$

$$(B''\,^1\Sigma_u^+) \quad (2\text{-}6)$$

$$(C\,^1\Pi_u) \quad (2\text{-}7)$$

$$(D\,^1\Pi_u) \quad (2\text{-}8)$$

$$(D'\,^1\Pi_u) \quad (2\text{-}9)$$

$$(E\,^1\Sigma_g^+) \quad (2\text{-}10)$$

$$(F\,^1\Sigma_g^+) \quad (2\text{-}11)$$

$$(H\,^1\Sigma_g^+) \quad (2\text{-}12)$$

$$(I\,^1\Pi_g) \quad (2\text{-}13)$$

$$(a\,^3\Sigma_g^+) \quad (2\text{-}14)$$

$$(b\,^3\Sigma_u^+) \quad (2\text{-}15)$$

$$(c\,^3\Pi_u) \quad (2\text{-}16)$$

$$(e\,^3\Sigma_u^+). \quad (2\text{-}17)$$

Reliability of the cross sections determined through optical measurements depends upon the calibration methods employed. In the excitation of H_2 accompanied with vacuum ultraviolet (VUV) photon emission, the cross sections are usually determined by normalizing relative photon intensities to a well-established Lyman-α emission cross section at a certain electron impact energy or to the cross sections calculated with the first Born approximation at high electron energies. Recently Shemansky *et al.*[18] reestablished the Lyman-α emission cross section at 100 eV to be 8.2×10^{-18} cm^2 as a standard. Thus the present cross sections based upon those recommended by Ajello *et al.*[17] are renormalized to this value (see further discussion on the newest results on Lyman-α emission cross section measurements in Sec. 2.3.2.). Similarly those of de Heer and Carriere[20] are again renormalized. On the other hand, Khakoo and Trajmar[19] determined the cross sections through electron energy-loss spectroscopy.

Theoretical calculations reported since 1970 for the electronic excitation are summarized in Table 1. Some elaborate calculations (i.e., by either a distorted-wave method or a close-coupling approximation) are shown and, where possible, compared with experimental data. In some cases, the agreement with experiments seems to be fairly good, yet a large discrepancy is sometimes observed. This reflects difficulties in the calculations of cross sections of the electronic excitation processes of molecules. Much work remains to be done in order to provide accurate theoretical data in the electronic excitation processes. The Born calculations, in principle, are thought to be reliable at higher energies, for example above a few hundreds of electron volts. Their reliability, however, should be confirmed experimentally.

The cross sections for excitation to various electronic states are shown in Figs. 6–14.

2.3. Dissociative Excitation of H_2

The dissociative excitation usually results in the emission of photons. Then the cross sections for dissociative exci-

Downloaded 24 Jun 2013 to 128.112.200.107. This article is copyrighted as indicated in the abstract. Reuse of AIP content is subject to the terms at: http://jpcrd.aip.org/about/rights_and_permissions

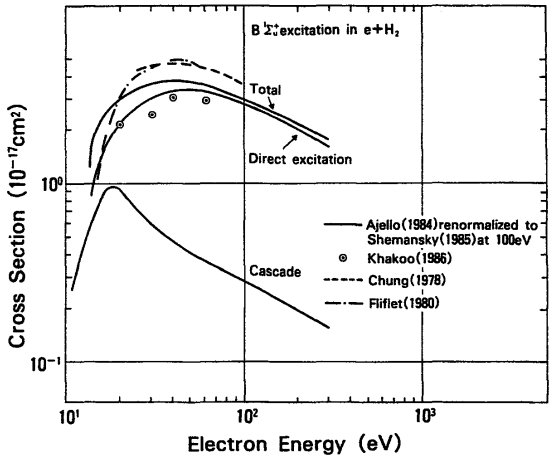


FIG. 6. Cross sections of electronic excitation to $B\ ^1\Sigma_u^+$.

tation can be determined through photon spectroscopy and the recommended cross sections are shown in Fig. 15. Note that these cross sections may include the contribution of dissociative ionization where one of the fragmented products results in the excited state atom (see Sec. 2.4).

2.3.1 Emission Cross Sections of Balmer-α, -β, -γ, and -δ Lines from H_2

$$e + H_2 \rightarrow e + H + H + h\nu(n = 3 \rightarrow 2) \ : \ \text{Balmer-}\alpha \qquad (2\text{-}18)$$

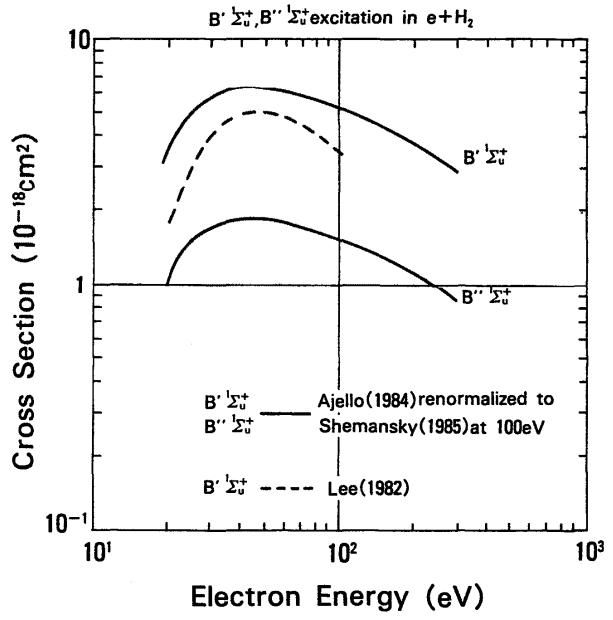


FIG. 7. Cross sections of electronic excitation to B' and $B''\ ^1\Sigma_u^+$.

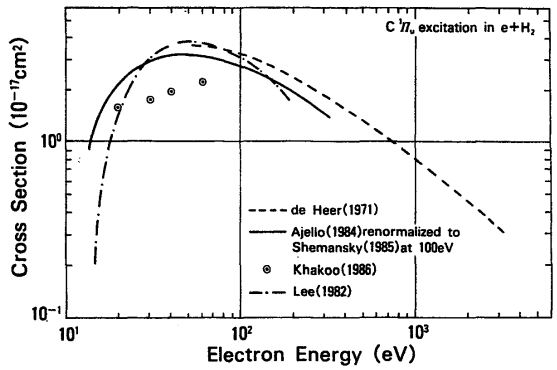


FIG. 8. Cross sections of electronic excitation to $C\ ^1\Pi_u$.

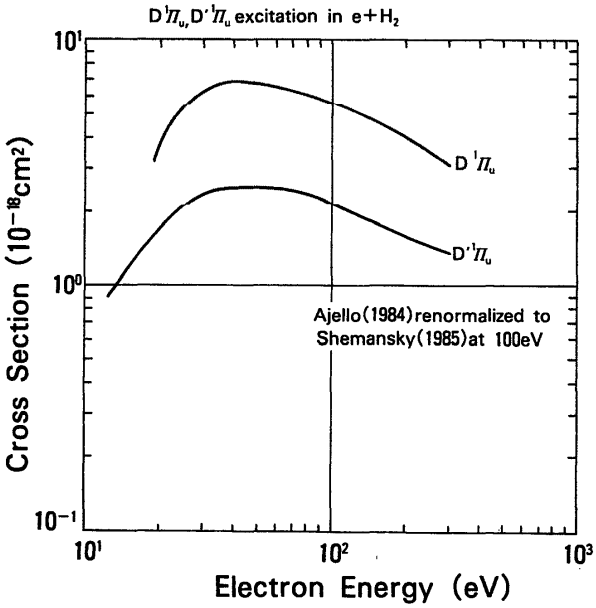


FIG. 9. Cross sections of electronic excitation to D and $D'\ ^1\Pi_u$.

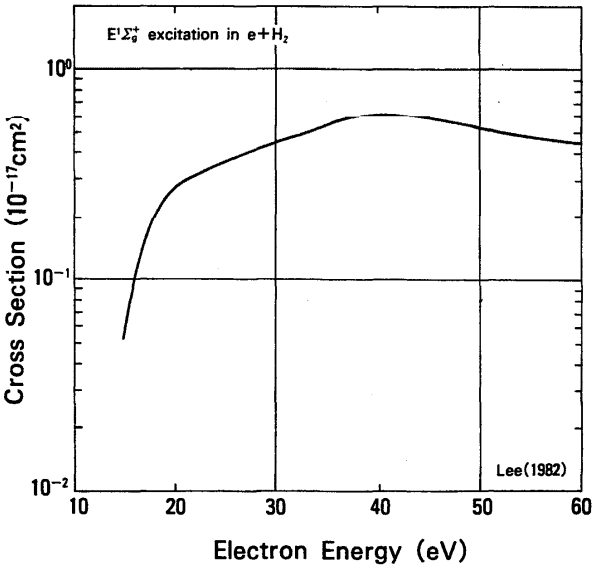


FIG. 10. Cross sections of electronic excitation to $E\ ^1\Sigma_g^+$.

Downloaded 24 Jun 2013 to 128.112.200.107. This article is copyrighted as indicated in the abstract. Reuse of AIP content is subject to the terms at: http://jpcrd.aip.org/about/rights_and_permissions

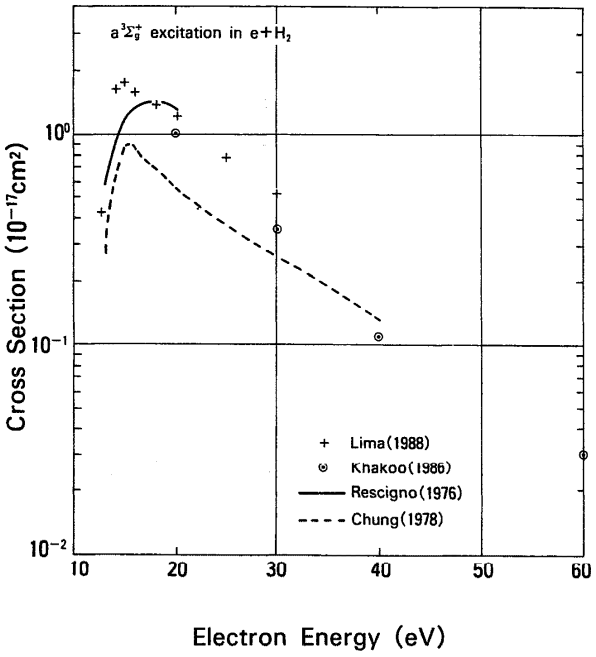


FIG. 11. Cross sections of electronic excitation to $a\ ^3\Sigma_g^+$.

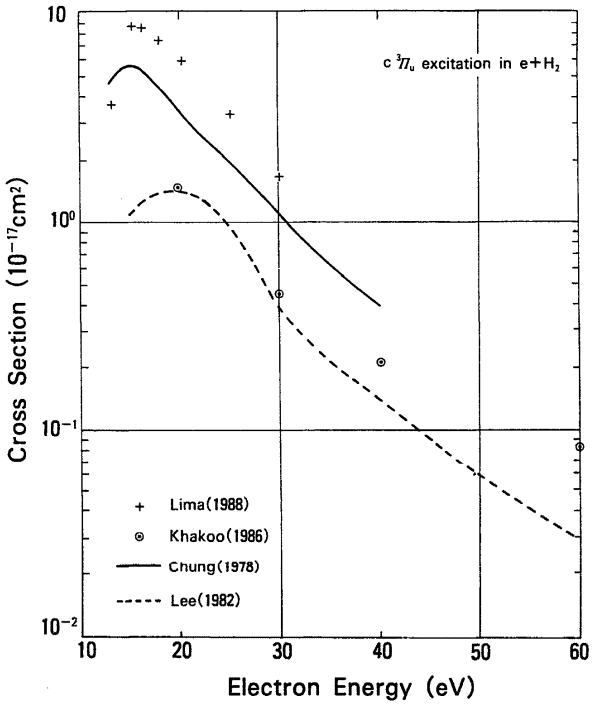


FIG. 13. Cross sections of electronic excitation to $c\ ^3\Pi_u$.

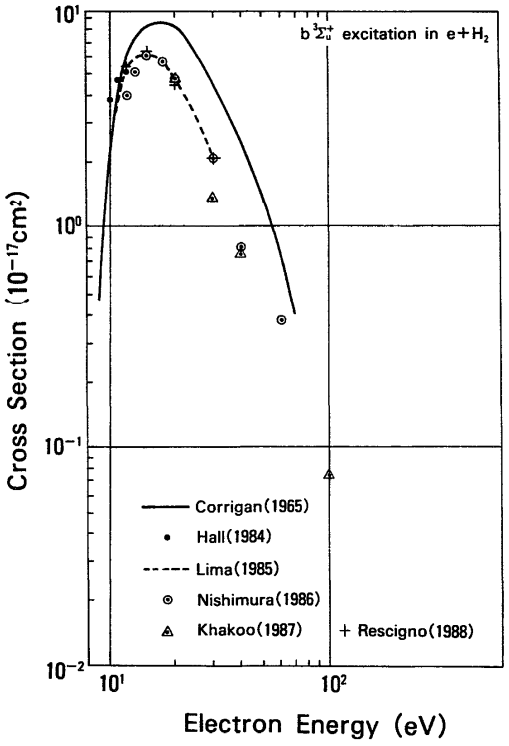


FIG. 12. Cross sections of electronic excitation to $b\ ^3\Sigma_u^+$.

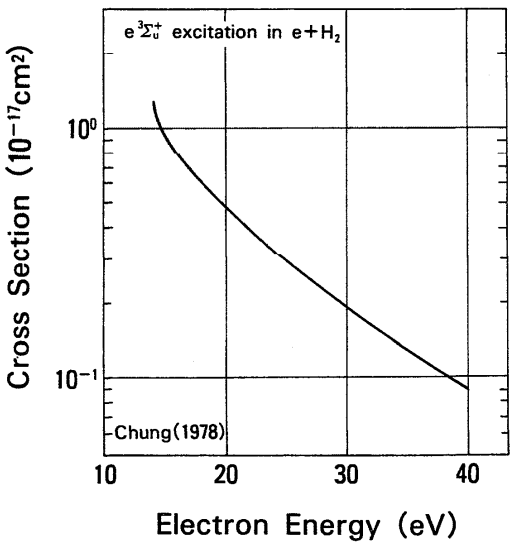


FIG. 14. Cross sections of electronic excitation to $e\ ^3\Sigma_u^+$.

Downloaded 24 Jun 2013 to 128.112.200.107. This article is copyrighted as indicated in the abstract. Reuse of AIP content is subject to the terms at: http://jpcrd.aip.org/about/rights_and_permissions

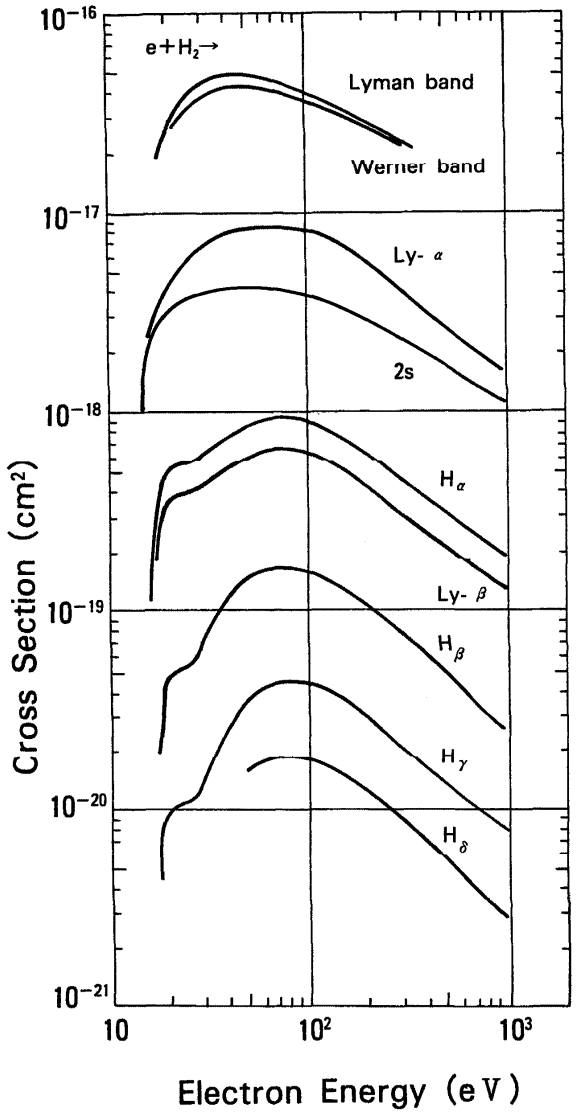


FIG. 15. Cross sections of photon emission for Lyman band, Werner band, Lyman-α, Lyman-β, 2s state, Balmer-α, -β, -γ and -δ lines (see Ref. 125).

$(n = 4 \rightarrow 2)$: Balmer-β (2-19)

$(n = 5 \rightarrow 2)$: Balmer-γ (2-20)

$(n = 6 \rightarrow 2)$: Balmer-δ. (2-21)

A number of the absolute emission cross sections for these lines resulting from hydrogen molecules have been reported.[49–52] The agreement among different measurements seems to be fairly good except for those by Vroom and de Heer[50] whose data at lower energies (below 150 eV) show slightly different behavior. These emission cross sections for D_2 molecules have also been measured. The cross sections ratios H_2/D_2 are varied with the electron energy. Those for Balmer-α line change from 1.4 at lower energies to 1.1 at higher energies (above 100 eV), whereas those for Balmer-β line change from 1.7 to 1.1 (above 60 eV). Because these lines fall in visible region, there are many applications which are based upon their observations.

2.3.2. Emission Cross Sections of Lyman-α and -β Lines from H_2

$e + H_2 \rightarrow e + H + H + h\nu(n = 2 \rightarrow 1)$: Lyman-α (2-22)

$(n = 3 \rightarrow 1)$: Lyman-β. (2-23)

Mumma and Zipf[53] determined their cross sections from ratios of those for the production of countable ultra violet radiations to those for excitation of Lyman-α line[54] whose absolute value was taken from that at 100 eV by Long *et al.*,[55] taking into account the contribution of molecular radiations transmitted through a LiF–O_2 filter.[56] Their value at 100 eV had been often used as a standard for determining the cross sections for other collision processes for more than 10 years.[17,57] However, recently Shemansky *et al.*[18] have re-examined carefully and redetermined the cross section to be $(8.2 \pm 1.2) \times 10^{-18}$ cm^2 at 100 eV. Thus all the measured cross sections based upon this old standard value, should be reduced by a factor of 0.69. Data shown in Fig. 15 taken from the original values by Mumma and Zipf,[53] Ajello *et al.*[17] and Vroom and de Heer[50] have been corrected in such a way. Note that some recent cross sections for Lyman-α line emission at 100 eV became available as follows (in units of 10^{-18} cm^2):

Shemansky *et al.*[18]	8.2 ± 1.2
Van Zyl *et al.*[58]	7.22 ± 1.36
Woolsey *et al.*[59]	7.13 ± 0.59
McPherson *et al.*[60]	6.57 ± 0.53.

All these values are still in agreement with each other within their claimed uncertainties. At the moment, however, it is difficult to find a particular preference. Therefore we have chosen the value by Shemansky *et al.* as a reference (tentatively). The cross sections shown in Fig. 15 are based upon the cross section at 100 eV by Shemansky *et al.*[18]

2.3.3. Cross Section for the Production of Metastable H(2s) Atoms from H_2

$e + H_2 \rightarrow e + H + H(2s)$ (2-24)

Vroom and de Heer[50] and later Möhlmann *et al.*[57] measured the production cross sections of H(2s) metastable state atoms by electron impact in the energy range from 50 eV, up to several thousands of eV by means of the electrostatic quenching technique. Another independent determination of the production cross sections of D(2s) metastable state was also reported by Cox and Smith.[61] In their experiments, the absolute scale was established on a purely experimental base, in contrast to Möhlmann *et al.*[57] whose measured relative values were normalized to that of Mumma and Zipf at 100 eV. The method Cox and Smith utilized depended upon the application of an rf field at the Lamb-shift frequency to quench the metastable state beams at the point of excitation. Their results are in good agreement with those by Mohlmann *et al.*[57], at a high-energy region. However, a con-

Downloaded 24 Jun 2013 to 128.112.200.107. This article is copyrighted as indicated in the abstract. Reuse of AIP content is subject to the terms at: http://jpcrd.aip.org/about/rights_and_permissions

siderable discrepancy is seen between both results in lower electron energy region. The cross sections for the production of H(2*s*) shown in Fig. 15 are deduced from the data by Cox and Smith for D_2 under the assumption that ratios of H(2*s*) from H_2 to D(2*s*) from D_2 are the same as observed by Vroom and de Heer[50] over the energy range investigated.

2.3.4. Cross Sections for Dissociative Excitation of H_2 to High Rydberg States

Shiavone *et al.*[62] determined their absolute excitation cross section for the production of atomic fragments in high Rydberg states at 100 eV. According to their measurements, the cross sections for the production of H(n) atoms are approximately given by $0.14\times10^{-16}/n^3$ (cm^2) for $n = 15$–80. They also reported the energy dependence of the cross sections which were compared with those obtained by Carnahan and Zipf[63] after correcting the radiative decay effect and other apparatus-dependent factors. The agreement was observed within the experimental uncertainties.

2.3.5. Emission Cross Sections of the Werner- and Lyman-band Systems from H_2

$$e + H_2 \rightarrow e + H_2^*(C\,^1\Pi_u \rightarrow X\,^1\Sigma_g^+) \text{ : Werner band,} \quad (2\text{-}25)$$

$$(B\,^1\Sigma_u^+ \rightarrow X\,^1\Sigma_g^+) \text{ : Lyman band.} \quad (2\text{-}26)$$

The cross sections for the emission of these bands were reported.[64,65] Though these processes are not dissociative, they seem to be relevant to comparison with other dissociative processes which result in photon emission.

Other types of experimental work which may clarify the nature of dissociative products will be discussed later (see Sec. 3).

2.4. Ionization and Dissociative Ionization of H_2

The following ionization processes are possible in electron impact on H_2 and their cross sections are shown in Fig. 16:

$$e + H_2 \rightarrow e + e + H_2^+, \quad (2\text{-}27)$$

$$\rightarrow e + e + H + H^+ \quad (2\text{-}28)$$

$$\rightarrow e + 2e + H_2^{2+} \rightarrow H^+ + H^+, \quad (2\text{-}29)$$

$$\rightarrow \text{total ion.} \quad (2\text{-}30)$$

The cross sections for Eqs. (2-27), (2-28), and (2-30), are given in the previous compilations.[66,67] Atomic hydrogens in Eq. (2-28) may be in the excited states, resulting in photon emission. Equation (2-30) represents total ion production including H_2^+ and H^+. The differentiation between the two Eqs. (2-28) and (2-29) can be made through coincidence technique. In fact, those for Eq. (2-29), namely, double ionization of hydrogen molecules resulting in dissociation into

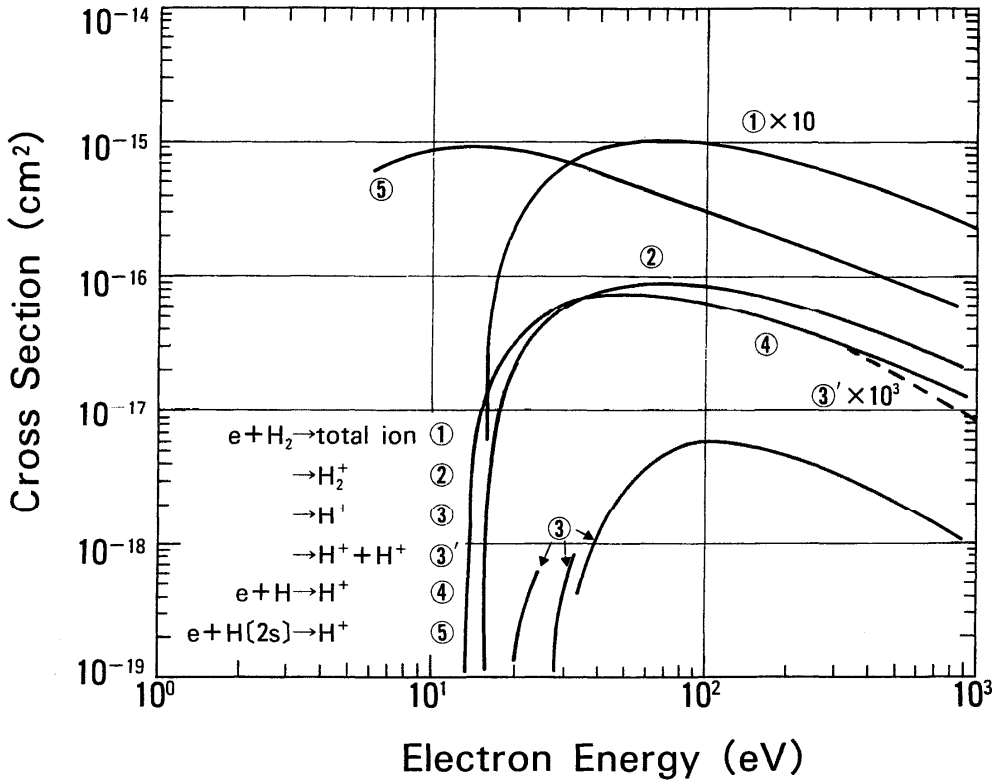


FIG. 16. Cross sections of the production for total ion, molecular hydrogen ions, protons and double protons. Those of proton production from H and H(2*s*) are also shown for comparison (see Ref. 125). Note that the short curves, for proton production at lower energies, correspond to the processes via $^2\Sigma_g$ (near-zero energy protons) and $^2\Sigma_u$ (repulsive state), respectively.

Downloaded 24 Jun 2013 to 128.112.200.107. This article is copyrighted as indicated in the abstract. Reuse of AIP content is subject to the terms at: http://jpcrd.aip.org/about/rights_and_permissions

two protons, have recently been measured over the energy range 400–1900 eV by Edwards *et al.*[68] who showed the ratios of cross sections of Eq. (2-29) to Eq. (2-27) are of the order of 10^{-3} and decrease with increasing the impact energy. The energy distributions of the product protons are peaked at about 9.4 eV (see Sec. 3.3).

For reference, the cross sections for ionization of atomic hydrogens in the ground and metastable states are also shown in Fig. 16:

$$e + H \rightarrow e + e + H^+, \quad (2\text{-}31)$$

$$e + H(2s) \rightarrow e + e + H^+. \quad (2\text{-}32)$$

2.5. Dissociative Attachment to H_2

$$e + H_2 \rightarrow H + H^-. \quad (2\text{-}33)$$

The cross sections for dissociative electron attachment are shown in Fig. 17, which is taken from the previous compilations.[67,69,70] Recently, it has been confirmed experimentally and theoretically that a small peak near the impact energy of 4 eV is strongly enhanced if H_2 molecules are in either vibrationally or rotationally excited states.[71,72,73] For example, the cross sections for H_2^* at the vibrationally excited state $v = 4$, are four orders of magnitude larger than those for the vibrationally ground state $v = 0$. See Table 2. This clearly indicates that vibrational (as well as rotational) excitation of molecules significantly increases the cross sections for dissociative attachment to H_2 molecules and the lowering of the threshold energies results in further enhanced cross sections near thresholds. This finding does contribute to the production of intense negative hydrogen ion beams (known as volume production) for application to, for example, fusion research.

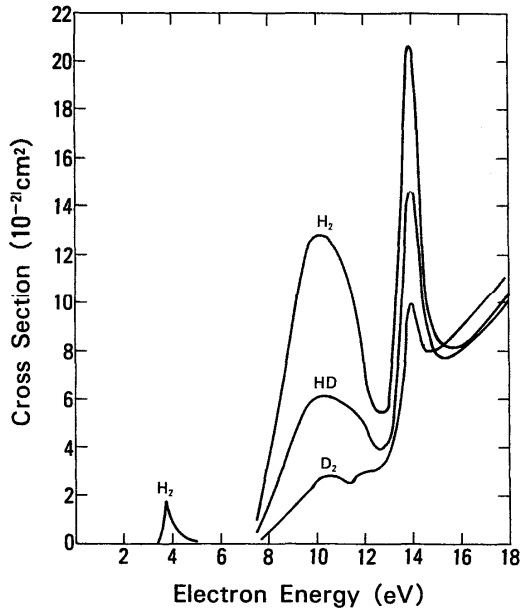


FIG. 17. Cross sections of dissociative attachment for HD and D_2 as well as H_2 (see Ref. 67).

TABLE 2. Dissociative-attachment cross sections near thresholds for several vibrational levels[72a].

v	E(eV)	σ(cm^2)
0	3.75	2.8(−21)
1	3.23	8.3(−20)
2	2.75	1.0(−18)
3	2.29	7.5(−18)
4	1.86	3.8(−17)
5	1.46	1.2(−18)
6	1.08	2.9(−18)
7	0.74	4.3(−18)
8	0.42	3.2(−18)
9	0.14	4.3(−18)

[a] Note: 2.8(−21) means 2.8×10^{-21}.

2.6. Collisions of H_2^+

In electron collisions with H_2^+ molecular ions, the cross sections for the following processes have been determined:

$$e + H_2^+ \rightarrow e + H^+ + H \quad \text{: dissociative excitation} \quad (2\text{-}34)$$

$$\rightarrow e + e + H^+H^+ \quad \text{: dissociative ionization} \quad (2\text{-}35)$$

$$\rightarrow H^+ + H^- \quad \text{: dissociative recombination} \quad (2\text{-}36)$$

$$\rightarrow H + H^* \quad \text{: dissociative recombination} \quad (2\text{-}37)$$

$$\rightarrow \text{total proton production.} \quad (2\text{-}38)$$

In these types of collision experiments, the cross-beam or merged-beam technique is often used. The measured cross sections for these processes are summarized in Fig. 18. It is important to note that H_2^+ beams used in experiments include various vibrationally excited states whose distributions may or may not follow the Frank–Condon principle, depending upon the type of ion sources used to produce ions, and the observed cross sections should be compared with great care. If all H_2^+ ions are in the vibrationally ground state, the cross sections should be small and, in fact, nearly one order of magnitude smaller than those shown in Fig. 18.[73]

The measured cross sections for proton production [Eq. (2-38)] are the sum of those for Eqs. (2-34), (2-35), and (2-36).[74–76] However, those for Eqs. (2-35)[77] and (2-36)[78] are more than one order of magnitude smaller than those for Eq. (2-34).[79]

The dissociative recombination process [Eq. (2-37)] resulting in two neutral atoms, either in the excited or ground state, has been extensively investigated experimentally and theoretically. Auerbach *et al.*[80] have shown rich structures in the cross-section curve, plotted as a function of the electron energy, under their high-resolution experiment. These sharp resonancelike structures are understood to be

Downloaded 24 Jun 2013 to 128.112.200.107. This article is copyrighted as indicated in the abstract. Reuse of AIP content is subject to the terms at: http://jpcrd.aip.org/about/rights_and_permissions

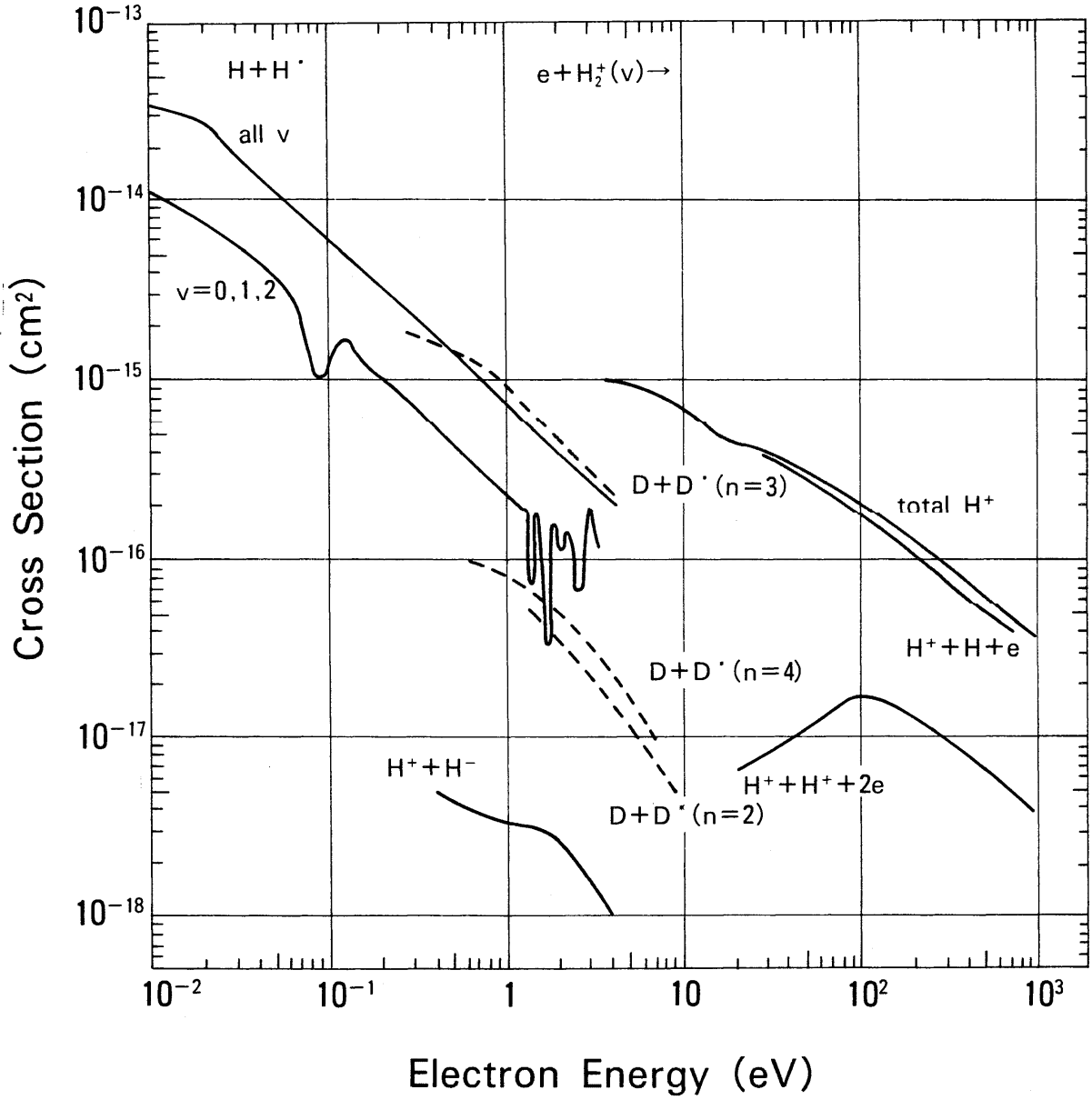


FIG. 18. Cross sections of electron collisions with $H(v)_2^+$ ions for the production of atomic hydrogens from all v, atomic hydrogens from $v = 0$, 1 and 2, $D + D^*(n = 2,3,4)$, total protons, $H^+ + H + e$, $H^+ + H^+ + 2e$ and $H^+ + H^-$.

due to indirect capture, into high-lying Rydberg states of neutral molecules.[81–83] These structures, however, are not shown in Fig. 18, except for a few pronounced structures observed in H_2^+ ions in relatively low vibrational states ($v = 0$–2). Instead, the smoothed lines for H_2^+ ions in low and relatively high vibrational states are drawn, both having roughly the $E^{-0.87}$-dependence over the energy range 0.01–4 eV. These data are roughly in agreement with those of Peart and Dolder[84] (beam) and of Mathur *et al.*[85] (ion-trapping) in the overlapped energy region. Recently Hus *et al.*[86] have measured the cross sections for H_2^+ ions in relatively well-defined low excited states which are found to be a factor of 2–4 smaller than those in Fig. 18.

The dissociative recombination resulting in deuterium atoms, in excited states such as

$$e + D_2^+ \rightarrow D + D^*(nl = 2p)^{87}, \quad (2\text{-}39)$$

$$\rightarrow D + D^*(n = 4)^{88}, \quad (2\text{-}40)$$

was investigated by observing the emitted photons (Lyman-α and Balmer-β lines). These cross sections are one order of magnitude smaller than total dissociative recombination cross sections measured by Peart and Dolder:[89]

$$e + D_2^+ \rightarrow D + D^*. \quad (2\text{-}41)$$

It should be noted that the dominant final-state atomic hydrogen product resulting from dissociative recombination

Downloaded 24 Jun 2013 to 128.112.200.107. This article is copyrighted as indicated in the abstract. Reuse of AIP content is subject to the terms at: http://jpcrd.aip.org/about/rights_and_permissions

process is expected to be $n = 3$ from the Landau–Zener model.[87]

2.7. Collision of H_3^+

The cross sections for the following processes involving H_3^+ ions have been measured:

$$e + H_3^+ \rightarrow H + H + H \quad \text{:dissociative recombination,} \quad (2\text{-}42)$$

$$\rightarrow H_2 + H \quad \text{:dissociative recombination,} \quad (2\text{-}43)$$

$$\rightarrow H_2^+ + H^- \quad \text{:dissociative recombination,} \quad (2\text{-}44)$$

$$\rightarrow e + H^+ + H + H \quad \text{:dissociative excitation.} \quad (2\text{-}45)$$

In Fig. 19 are shown the cross sections for these processes. The sum of the cross sections for Eqs. (2-42) and (2-43) was measured with the crossed-beam, merged-beam, ion-trapping or flowing-afterglow technique.[80,85,90–93] Comparing these cross sections, it should be borne in mind that the cross sections are strongly dependent upon the internal energy of the parent H_3^+ ions, as in H_2^+ ions (see Sec. 2.6.). Particularly, the distributions of vibrationally excited states of H_3^+ ions influence significantly the observed cross sections. This is clearly seen in Fig. 19 where the observed cross sections are in significant disagreement among different authors who used H_3^+ ions, produced in different types of ion sources [see curves (1) and (2) of Fig. 19].

Recently, Hus *et al.*[94] checked the cross sections dependent upon the initial electronic states of H_3^+ ions and found that ions produced in an rf ion source have the largest cross sections, similar to those shown in Fig. 19, whereas the cross sections of ions produced in a trapped ion source are smaller by an order of magnitude, compared with those in rf ion source. Similarly, the cross sections obtained using the flow-

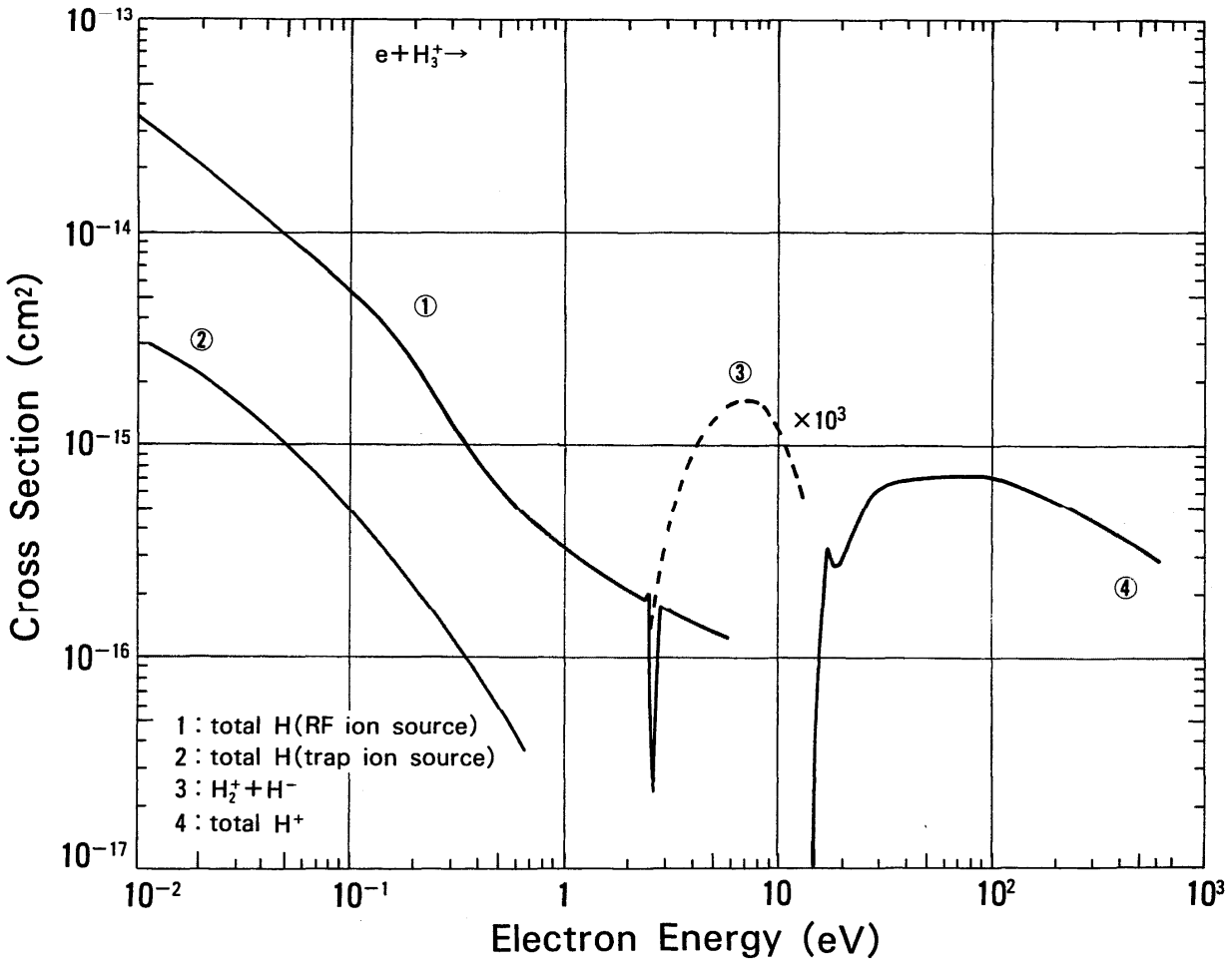


FIG. 19. Cross sections of electron collisions with H_3^+ ions for the production of total atomic hydrogens (rf-ion source and trap-ion source), total protons and $H_2^+ + H^-$. It should be noted that the difference between curves (1) and (2) in the production cross sections for atomic hydrogens is believed to be due to different electronic states of H_3^+ ions produced in different ion sources. See the text for more detailed discussion.

Downloaded 24 Jun 2013 to 128.112.200.107. This article is copyrighted as indicated in the abstract. Reuse of AIP content is subject to the terms at: http://jpcrd.aip.org/about/rights_and_permissions

ing-afterglow/Langmuir probe method[93] were found to be fairly small, compared with those obtained with the merged-beam method, shown in Fig. 19. These facts probably indicate that H_3^+ ions in their beam are almost relaxed to the vibrationally ground state, through collisions in swarms.

On the other hand, Amano[95] has recently determined the rate constant for dissociative recombination of H_3^+ ions with a particular rotational level ($J=3$, $K=3$) in the ground vibrational state (1.8×10^{-7} cm^3/s at 210 K) which is larger by an order of magnitude than that of trapped ions by Hus *et al.*[94] (2×10^{-8} cm^3/s) mentioned above. At liquid helium temperatures, the rate constant is found to be extremely small, being less than 10^{-11} cm^3/s, suggesting that H_3^+ ions in the ground vibrational state do not react with slow electrons. Thus significant discrepancies remain to be investigated.

Mitchell *et al.*[96] observed a significant isotope effect in the cross sections (those for H_3^+ are about three times those for D_3^+ ions) at low energies and explained that this effect is due to the lower vibrational frequency of D_3^+ ions. But this difference almost disappears at energies above 5 eV. It should also be noted that there are rich structures in the cross sections at higher energies when high-energy resolution measurements were made.[80] Only a significant oscillation at $\cong$3 eV is shown in Fig. 19.

Recently Mitchell *et al.*[97] distinguished two channels in the dissociative recombination Eqs. (2-42) and (2-43) and found that Eq. (2-42) is dominant over Eq. (2-43) by a factor of 2–3, over the energy range 0.01–0.5 eV. The cross sections for Eq. (2-44), resulting in the production of negative hydrogen ions, are small,[98] as shown in Fig. 19 (multiplied by 10^3). The cross sections for proton production, mainly due to Eq. (2-45), show a clear threshold around 15 eV.[99,100] Some theoretical aspects on dissociative recombination in $e + H_3^+$ collision processes at low temperatures, are given by Michels and Hobbs.[101]

As mentioned above, it is quite important to note that the dissociative recombination cross sections depend strongly upon the internal energy of molecular ions and, when they are used, great care should be exercised if molecular ions are in different electronic states such as those in plasmas.

3. Characteristics of the Products from H_2

3.1. Hydrogen Atoms from Dissociative Excitation/Ionization of H_2

A number of data involving production of atomic hydrogens, either in the ground state or the excited states, have been obtained. Characteristics of atomic hydrogen can be understood qualitatively through the potential energy diagram of H_2 (see Fig. 1).

3.1.1. Hydrogen Atoms in the Ground State

Total cross sections for the production of two atoms, both in the ground state H(1*s*), via dissociative excitation process through the lowest repulsive $b\,^3\Sigma_u^+$ state

$$e + H_2 \rightarrow e + H(1s) + H(1s), \qquad (3\text{-}1)$$

are known (see Figs. 2 and 12)[22,23,102] and this process occurs dominantly at low-energy region. In addition to this process, with increasing the electron energy, hydrogen atoms in the ground state are produced through a number of singly excited (or ionized) states. From the lowest excited states of H_2, two kinds of H(1*s*) atoms with different energies are produced: one is the near-zero energy atoms from the attractive $1s\sigma\,^2\Sigma_g^+$ state, resulting in dissociation into $H^+ + H(1s)$ and the other relatively high-energy atom ($\cong$7 eV) from the corresponding repulsive $2p\sigma_u\,^2\Sigma_u^+$ state. In between there are a series of different channels contributing to the production of H(1*s*) through $H(1s) + H^*(nl)$ excitation. Only little is known on the behavior of H(1*s*) atoms produced through dissociation of H_2 molecules. In fact, because of difficulties in detecting atoms in the ground state, their energy distributions and angular distributions have not yet been investigated in detail, though their average kinetic energy of both atoms is roughly estimated to be $\sim$2–3 eV each from the electron energy-loss spectrum or the potential energy diagram of H_2 shown in Fig. 1 and atoms produced are expected to be isotropically distributed. Very recently, a technique has been developed for measuring the energy distributions of the dissociated ground state hydrogen atoms based upon the deflection in nonuniform magnetic fields, due to the magnetic moment.[103]

3.1.2. Atoms in the Excited States

If the product hydrogen atoms are in the excited states, they can decay into lower states with the emission of photons. By observing the Doppler profiles of photons from these atoms, the kinetic energy distributions can be known[104] (see Fig. 20). At low electron energies, only the unshifted peak is observed, meanwhile the combined peak composed of two types, one being the unshifted and the other broadened, is seen at higher electron energies.

The energy distributions of the metastable H(2*s*) atoms from the process

$$e + H_2 \rightarrow e + H_2^{**} \rightarrow e + H^*(2s) + H^*(nl), \qquad (3\text{-}2)$$

were investigated by Leventhal *et al.*[105] who observed three components with the average energy of 0.21 ± 0.02, 2.3 ± 0.5 and 4.4 ± 0.9 eV at the impact energy of 60 eV at 13° with respect to the electron beam direction. They found that the slow component does not change with the observing angle, meanwhile the fast components do change with the angle. Thus at 90° only a single peak corresponding to the energy of 4.7 ± 0.7 eV, could be observed. More detailed analysis was made by Spezeski *et al.*[106] The slow component is understood to originate from the attractive, singly excited states such as $B\,^1\Sigma_u^+$, $B'\,^1\Sigma_u^+$, $e\,^3\Sigma_u^+$, $E\,^1\Sigma_g^+$ and $a\,^3\Sigma_g^+$. On the other hand, the fast components are found to originate from repulsive, doubly excited states. It is inferred from their results that at least two repulsive states, with different symmetries such as $(2p\sigma)$, $(2s\sigma)$ $^{1,3}\Sigma_u^+$ states, contribute to the fast component. The angular distributions of H(2*s*) atoms have also been reported.[107]

The following particular process:

$$e + H_2 \rightarrow e + e + H^+ + H^*(2s), \qquad (3\text{-}3)$$

has been investigated through coincidence technique

Downloaded 24 Jun 2013 to 128.112.200.107. This article is copyrighted as indicated in the abstract. Reuse of AIP content is subject to the terms at: http://jpcrd.aip.org/about/rights_and_permissions

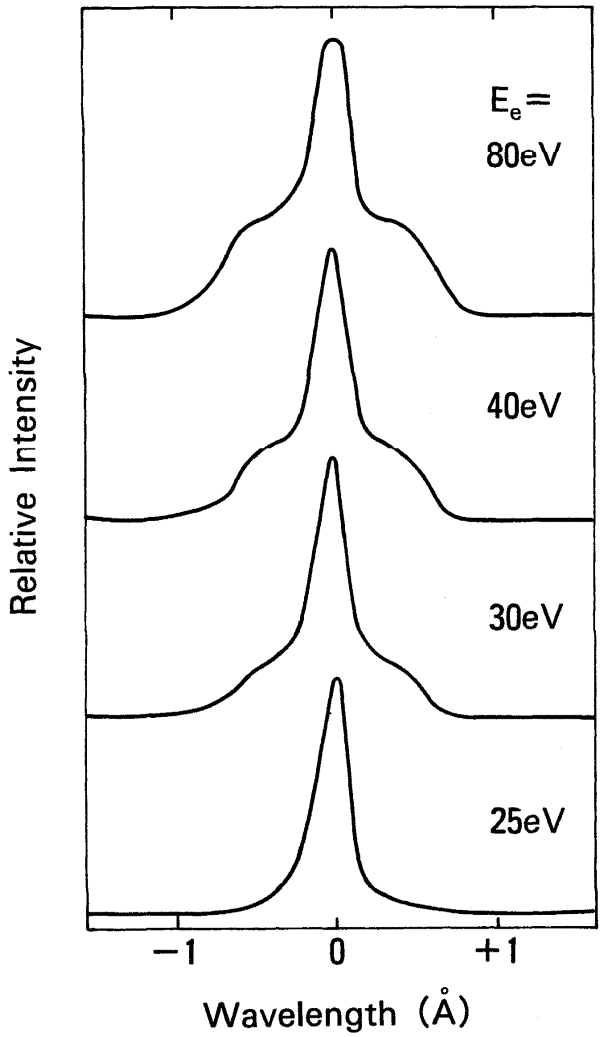


FIG. 20. Doppler-shifted spectral shapes of Balmer-β line as a function of the electron impact energy (see Ref. 104).

between proton and quenched Lyman-α radiation.[108] The kinetic energy of H(2s) atoms is estimated to be ~4–8 eV with a maximum at 5.8 eV, in agreement with the work of Leventhal *et al.*[105] and it was concluded that these H(2s) atoms originate mostly from $2s\sigma_g$ with a slight contribution of $3p\sigma_u$ state. No absolute cross section for this process, however, was determined. The state-selective dissociation process

$$e + D_2 \rightarrow e + D^*(2p) + D^*(2p) \quad (3\text{-}4)$$

has been studied through coincidence between two Lyman-α radiations. These atoms in the 2p state originate from the doubly excited states via dissociation. The cross sections for the process is estimated to be 5×10^{-20} cm^2 with the uncertainty of a factor of 2 at 200 eV.[109] This small cross section can be understood from the fact that there are other competing exit channels such as autoionization and singly excited Rydberg states. Hydrogen atoms in the $n = 3$ states produced through the process

$$e + H_2 \rightarrow e + H_2^{**} \rightarrow e + H^*(n = 3) + H^*(nl) \quad (3\text{-}5)$$

are found, by observing Balmer-α radiations, to have two components in their energy distribution[110]: one is the near-zero energy with the average energy of 0.2 eV produced through predissociation of vibrationally excited states such as $1s\sigma_g$ state or Rydberg states which are directly dissociated and the other one relatively high energy of 7 eV which is produced through the repulsive doubly-excited states such as $2p\sigma_u$. It is interesting to note that these Balmer lines originate mainly from 3s and 3d states.[111] However, no quantitative measurement of this process has been reported. By observing Balmer-β radiations, similar investigations on the production mechanisms of H($n = 4$) atoms

$$e \rightarrow H_2 \rightarrow e + H_2^{**} \rightarrow e + H^*(n = 4) + H^*(nl) \quad (3\text{-}6)$$

can be made and it is found that there are three components at ≅0, 4 and 8 eV, whose threshold energies are 17.1, 24 and 27 eV, respectively.[112] Their production mechanisms are very similar to those of H($n = 3$) atoms. The situation is also quite similar in the production of H($n = 5$) atoms

$$e + H_2 \rightarrow e + H_2^{**} \rightarrow e + H^*(n = 5) + H^*(nl) \quad (3\text{-}7)$$

where three components are observed at the energy of ≅0, 4 and 7–8 eV, with the threshold energies of 17.5, 26 and 26 eV, respectively. A peak of high-energy component shifts from ~4 eV to 8 eV with increasing the electron energy,[113] suggesting that many channels contribute to the production of atoms. In principle, the angular distributions of their intensities and of their energy can be inferred from measurements of Doppler profiles of photons, as a function of the observing angle.[114] In fact, the Doppler profiles are found to be dependent not only upon the kinetic energy and angular distributions of these atoms but also upon the polarization of the photons.[114]

3.2. Protons from Dissociative Ionization of H_2

Proton production from the dissociative ionization of H_2 can be understood qualitatively from Fig. 21 where only some relevant potential-energy diagrams of H_2, H_2^+ and H_2^{2+} are shown.[115] Looking at Fig. 21, the expected energy distributions of protons from the process

$$e + H_2 \rightarrow e + e + H_2^{**} \rightarrow e + e + H^+ + H^*(nl) \quad (3\text{-}8)$$

can be inferred as shown on the left-hand side of Fig. 21. There are two main components: one is protons from transition of $^2\Sigma_g^+$ of H_2^+ and has peak intensity at near-zero energy and the other is protons from a number of the repulsive states of the excited H_2^{+*} ions as well as from the repulsive $^2\Sigma_u^+$ state of H_2^+ and therefore has broad energy distributions peaked at the energy of ~8 eV.

At the collision energy lower than the threshold of transitions to $^2\Sigma_u^+$ state, protons come mainly from $^2\Sigma_g^+$ state. Crowe and McConkey[116] determined ratios of protons to H_2^+ ions which increase roughly, linearly with the electron collision energy from zero at the threshold of 18 eV up to 0.015 at 25 eV, approaching ratios in photon impact which sharply increase and become flat above the threshold (see Fig. 22).

Rapp *et al.*[117] determined fractions of protons having

Downloaded 24 Jun 2013 to 128.112.200.107. This article is copyrighted as indicated in the abstract. Reuse of AIP content is subject to the terms at: http://jpcrd.aip.org/about/rights_and_permissions

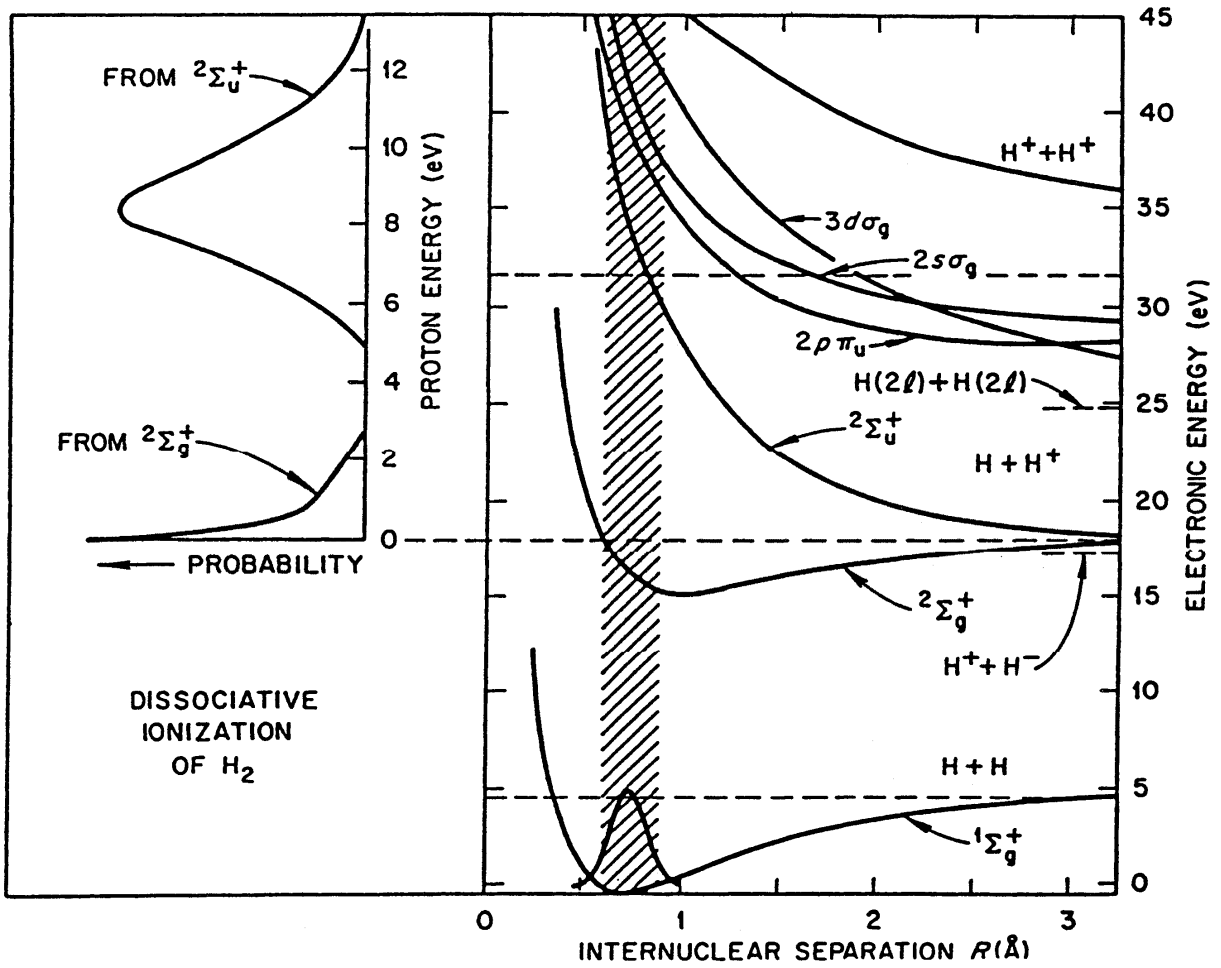


FIG. 21. Potential energy curves of H_2, H_2^+ and H_2^{2+} and the expected energy distributions of protons produced via $^2\Sigma_g^+$ and $^2\Sigma_u^+$ states of H_2^+ in dissociative ionization of H_2 (see Ref. 115).

the energy higher than 0.25 eV by applying the retarding potential and found that these high-energy protons ($E_p > 0.25$ eV) consist of roughly 7% (maximum) of total ions (mainly H_2^+) at the collision energy of 120 eV, decreasing with increasing the collision energy (see Fig. 23 and Fig. 16).

The angular distributions of the zero-energy protons are essentially isotropic up to the electron collision energy of

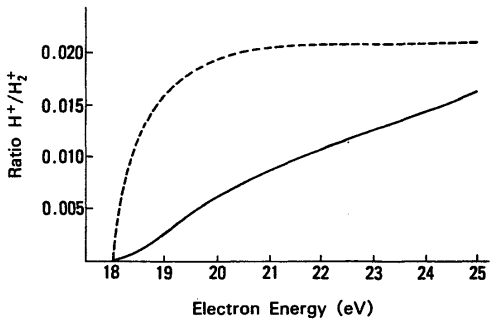


FIG. 22. Ratios of H^+/H_2^+ in electron impact. The solid curve shows these ratios in electron impact whereas the dashed curve represents those in photon impact (see Ref. 116).

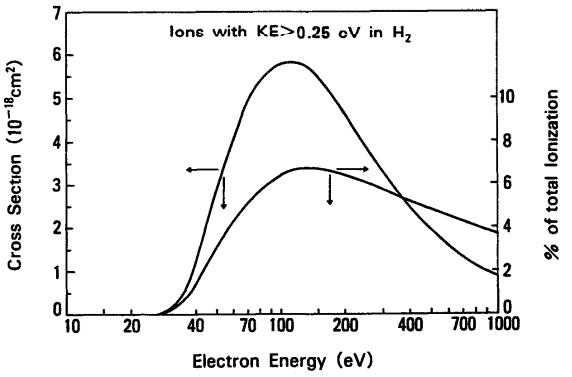


FIG. 23. Cross sections of production of protons with the energy above 0.25 eV and their fractions (see Ref. 117).

Downloaded 24 Jun 2013 to 128.112.200.107. This article is copyrighted as indicated in the abstract. Reuse of AIP content is subject to the terms at: http://jpcrd.aip.org/about/rights_and_permissions

25 eV, with a forward–backward asymmetry due to momentum transfer ($\pm$ 20% at 22.3 eV with respect to that at 90°), agreeing with the Dunn prediction for $\Sigma_g^+ - \Sigma_g^+$ transitions.[118] As the energy of protons from $^2\Sigma_g^+$ state is of the order of rotational energy of H_2 molecules ($\cong$0.02 eV), the observed angular distributions of the zero-energy protons could be smeared out and become isotropic, even if initially anisotropic. As their energy is also comparable to thermal energy of H_2 molecules, again the initial anisotropy, if any, tends to be smeared out.

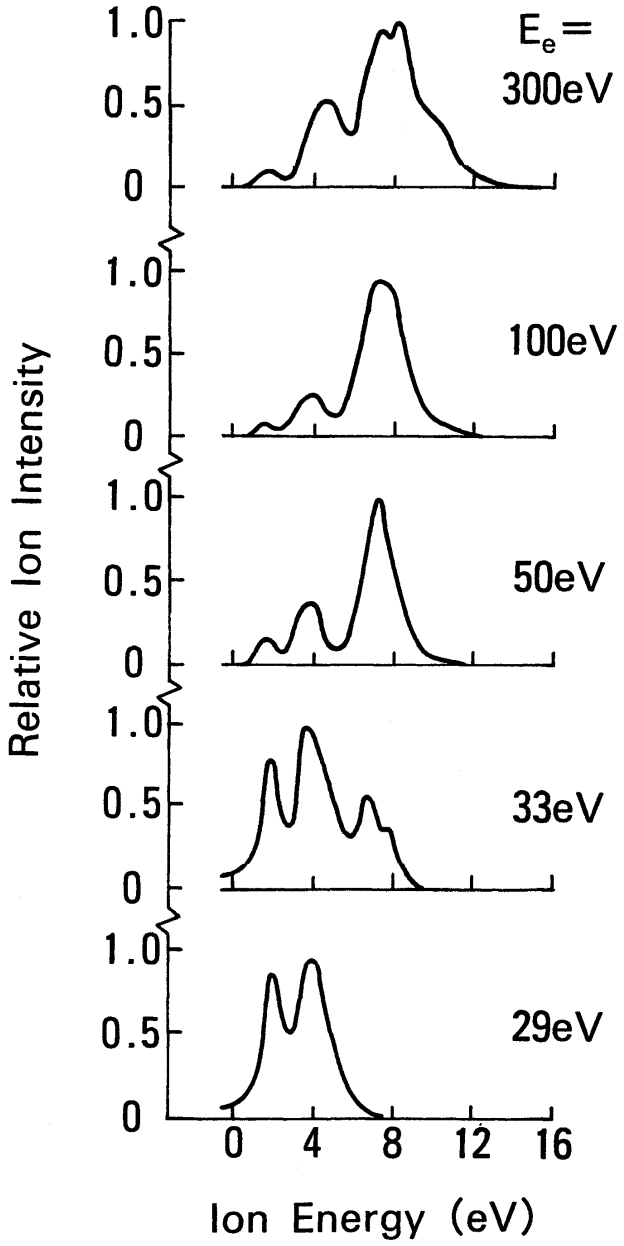


FIG. 24. Proton energy spectra at different electron impact energies. Note that the spectral shapes change with the electron impact energy (see Ref. 119).

The energy distributions of high-energy protons from H_2 were measured by Crowe and McConkey[119] who revealed a number of peaks at the energy of 1, 2, 4, and 8 eV. The spectrum, where all the peaks seem to have shoulders, suggests that a number of channels located between $^2\Sigma_g^+$ and $^2\Sigma_u^+$ states might contribute to the production of protons. The intensities of these peaks change significantly, with the electron impact energy (see Fig. 24). At the energies higher than 50 eV, the peak at 8 eV becomes dominant, though the detailed energy distributions of protons depend on the observing angle. It should be noted, however, that these structures in the energy spectrum observed by Crowe and McConkey were not confirmed either by Kallman[120] or most recently by Khakoo and Srivastava.[121] Also, it is noted that protons with near-zero energies are very much suppressed in measurements of Crowe and McConkey.

As mentioned above, the angular distributions of protons are dependent upon the electron collision energy and also the proton energy itself (see Fig. 25).[120] Generally speaking, at low electron energies, the distributions show the forward–backward enhancement with a minimum at 90° and at the energy $\sim$100 eV become nearly isotropic and, then, the intensities become maximum at 90° with a slight forward–backward reduction at further higher energies. Some examples are shown in Fig. 25, where the angular distributions of protons with the energy of 8 eV are given for different collision energies over 50–1500 eV.[115] These observed distributions can be understood well by the Born calculations of Zare.[122] According to his calculations, the anisotropy is found to be large for high-energy protons and confirmed experimentally, as seen in Fig. 26.[120] This is supported by van Brunt[123] who observed the variation of the angular distributions in proton energy at different angles, suggesting that the peak at 8 eV should have stronger anisotropy, compared with those of lower energy protons. Similar

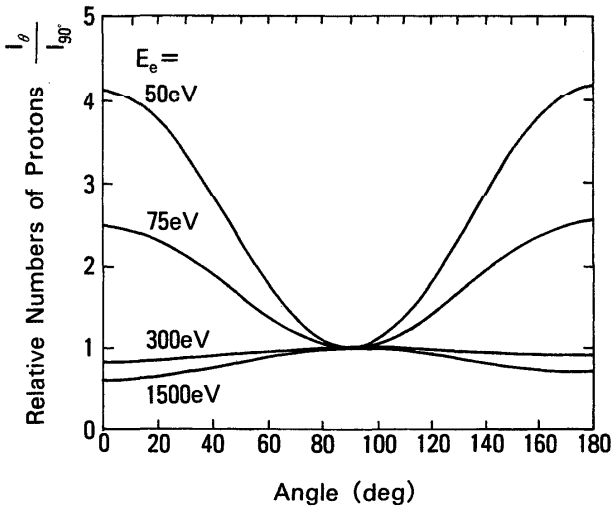


FIG. 25. Relative angular distributions of 8.6 eV protons produced from H_2 in various electron impact energies (see Ref. 115).

Downloaded 24 Jun 2013 to 128.112.200.107. This article is copyrighted as indicated in the abstract. Reuse of AIP content is subject to the terms at: http://jpcrd.aip.org/about/rights_and_permissions

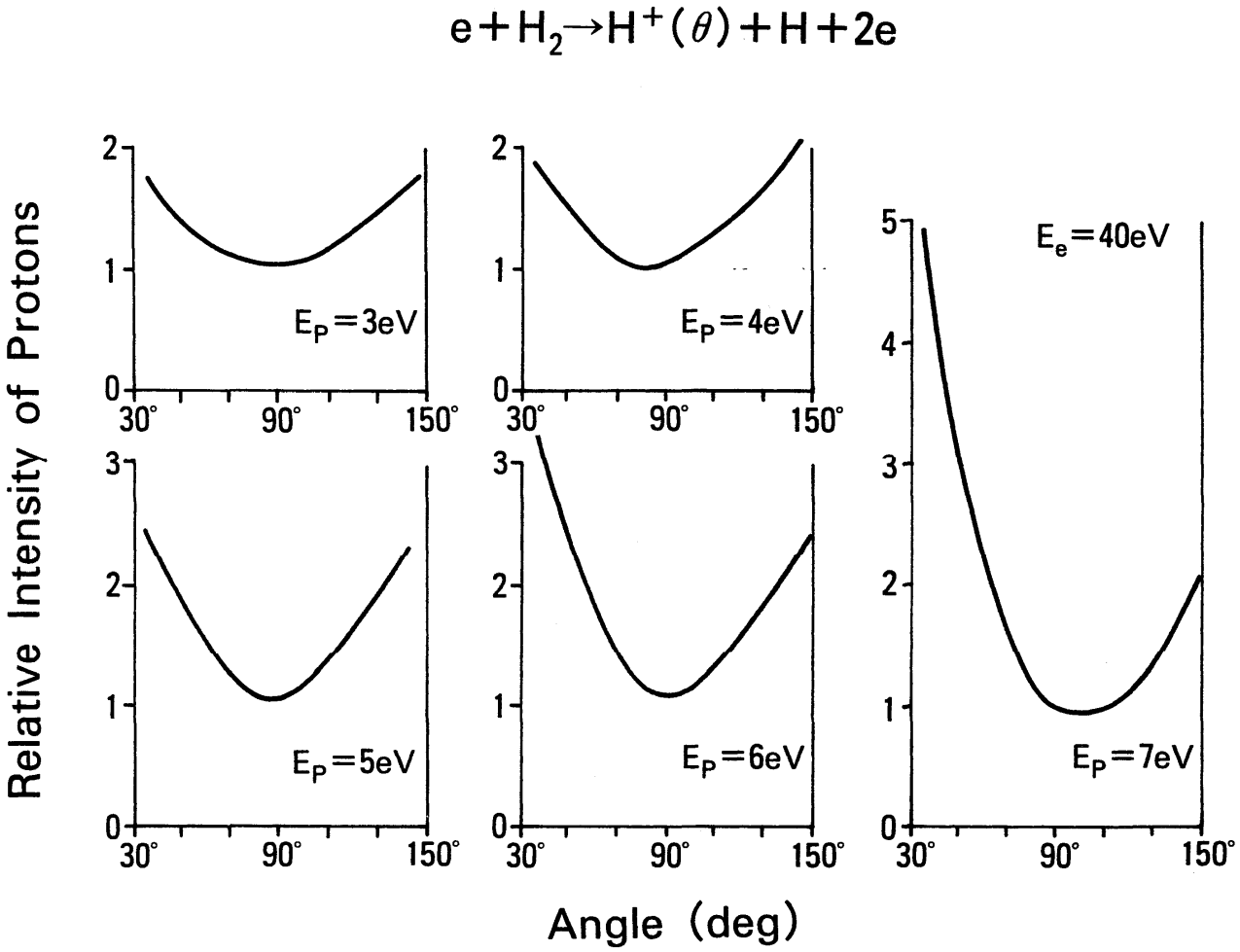


FIG. 26. Angular anisotropy of protons with the energy of 3, 4, 5, 6 and 7 eV at the electron impact energy of 40 eV (see Ref. 120).

observations were also reported by Crowe and McConkey,[119] whose spectra indicated that peaks with lower energies (2 and 4 eV) are relatively isotropic.

3.3. Protons from Double Ionization of H_2

Doubly charged molecular ions H_2^+ are promptly dissociated through the repulsive $2p\sigma$ state:

$$e + H_2 \rightarrow e + 2e + H_2^{2+} \rightarrow H^+ + H^+. \qquad (3\text{-}9) = (2\text{-}29)$$

Then, two resultant protons are emitted into the opposite directions with high initial kinetic energy. Coincidence measurements between two protons provide information on this process. The measured energies of these protons range from 6 to 14 eV peaked at 9.4 eV, as shown in Fig. 27,[124] and are found not to change very much over the collision energy of 0.5 to 1.0 keV, as expected. The cross sections of double ionization of H_2, already shown in Fig. 16,[68] are found to be roughly three orders of magnitude smaller than those of single ionization.

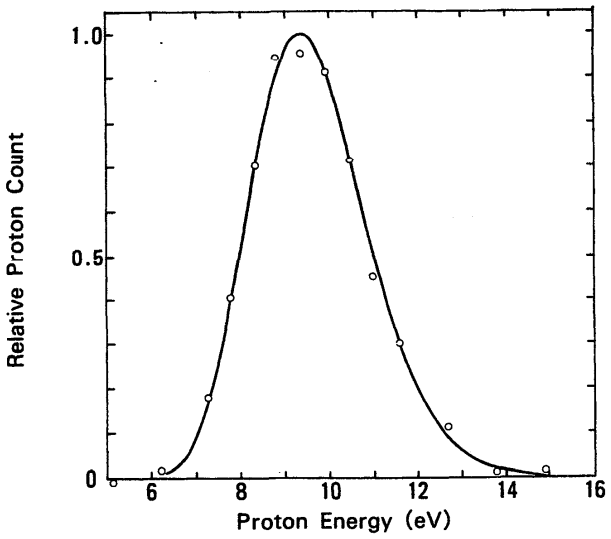


FIG. 27. Energy distribution of protons from doubly ionized hydrogen molecules in electron impact (see Ref. 124). The open circles denote the observed data, meanwhile the solid line represents the calculated distribution.

Downloaded 24 Jun 2013 to 128.112.200.107. This article is copyrighted as indicated in the abstract. Reuse of AIP content is subject to the terms at: http://jpcrd.aip.org/about/rights_and_permissions

4. Concluding Remarks and Comments on Future Work

We have shown important data related with hydrogen molecules and molecular ions in colliding with electrons which have been taken mostly from our previous reports[125,126] with the addition of new data reported recently. Generally, a large body of data are now available, yet some are still not reliable or not available even though they seem to be the most elemental for understanding collisions involving hydrogen molecules or molecular ions. Among the many items to be determined, some of the most important are listed in the following:

(i) Cross sections for the collisions of the state-selected molecules are very limited presently and systematic measurements should be performed.

(ii) Cross sections involving molecular ions are strongly dependent upon and varied, sometimes, orders of magnitude with their internal energy. Therefore, collisions of molecular ions, with the fully specified internal energy states should be investigated.

(iii) Energy distributions of protons and ground-/excited-state atoms produced in various processes are still not reliable. Systematic measurements of their energy are needed. It is particularly important to note that the precise energy distributions of the ground-state atoms, one of the most basic data involving molecular dissociation, have never been measured yet.

(iv) Information on angular distributions of the products, protons, atoms or photons, are still scarce.

In many applications, information on electrons scattered or produced is also important. In particular, in understanding the exciting or ionizing phenomena of matters such as those in radiation research, not only total cross sections but also energy distributions, as well as angular distributions (so-called singly or doubly differential cross sections) of electrons are essential.[127,128] These differential cross sections are known to depend upon a number of collision parameters, such as collision energy or types of collisions, and are indeed given in most of the experimental as well as theoretical studies discussed above. Because they have too many variations, they are not included in the present work.

5. Acknowledgment

The authors would like to thank Prof. K. Takayanagi for his support and encouragement, toward the present work.

6. References

[1]S. Trajmar, D. F. Register, and A. Chutjian, Phys. Report **97**, 219 (1983).
[2]G. Csanak, D. C. Cartwright, S. K. Srivastava, and S. Trajmar, in *Electron-Molecule Interactions and Their Applications* (edited by L. G. Christophrou, Academic Press, 1984), Vol. 1; S. Trajmar and D. C. Cartwright, ibid., p. 155; J. W. McConkey, S. Trajmar, and G. C. M. King, Comm. At. Mol. Phys. **22**, 17 (1988).
[3]R. K. Janev, W. D. Langer, K. Evans, Jr., and D. E. Post, *Atomic and Molecular Processes in Hydrogen-Helium Plasmas* (Springer Verlag, 1988).
[4]I. Shimamura, Scientific Paper of the Institute of Physica and Chemical Research **82**, 1 (1989).
[5]T. E. Sharp, At. Data Tables **2**, 119 (1971).
[6]M. Hayashi, IPPJ-AM-19 (Institute of Plasma Physics, Nagoya University, Nagoya, 1981).
[7]B. van Wingerden, E. Weigold, and F. J. Nygaard, J. Phys. B **10**, 1345 (1977).
[8]T. W. Shyn and W. E. Sharp, Phys. Rev. A **24**, 1734 (1981).
[9]H. Nishimura, A. Danjo, and H. Sugahara, J. Phys. Soc. Japan **54**, 1757 (1985).
[10]G. Dalba, P. Fornasini, I. Lazzizzera, G. Ranieri, and A. Zecca, J. Phys. B **13**, 2839 (1980); J. Furst, M. Mahgerefteh, and D. E. Golden, Phys. Rev. A **30**, 2256 (1984).
[11]R. W. Crompton, D. K. Gibson, and A. I. McIntosh, Aust. J. Phys. **22**, 715 (1969).
[12]D. K. Gibson, Aust. J. Phys. **23**, 683 (1979).
[13]F. Linder and H. Schmidt, Z. Naturforsch. **269**, 1603 (1971).
[14]S. J. Schulz, Phys. Rev. **135**, A988 (1964).
[15]H. Ehrhardt, L. Langhans, F. Linder, and H. S. Taylor, Phys. Rev. **173**, 222 (1969).
[16]M. Allan, J. Phys. B **18**, L451 (1985).
[17]J. M. Ajello, D. E. Shemansky, T. L. Kwok, and Y. L. Yung, Phys. Rev. A **29**, 636 (1984).
[18]D. E. Shemansky, J. M. Ajello, and D. T. Hall, Astrophys. J. **296**, 765 (1985).
[19]M. A. Khakoo and S. Trajmar, Phys. Rev. A **34**, 146 (1986).
[20]F. J. de Heer and J. D. Carriere, J. Chem. Phys. **55**, 3829 (1971).
[21]S. J. B. Corrigan, J. Chem. Phys. **43**, 4381 (1965).
[22]R. I. Hall and L. Andric, J. Phys. B **17**, 3815 (1984).
[23]H. Nishimura and A. Danjo, J. Phys. Soc. Japan **55**, 3031 (1987).
[24]N. F. Lane, Rev. Mod. Phys. **52**, 29 (1980); N. F. Lane, in *Electronic and Atomic Collisions*, edited by J. Eichler, I. V. Hertel, and N. Stolterfoht (Elsevier, 1984), p. 127.
[25]A. Klonover and U. Kaldor, J. Phys. B **12**, 3797 (1979).
[26]M. A. Morrison, A. N. Feldt, and B. C. Saha, Phys. Rev. A **30**, 2811 (1984).
[27]M. A. Morrison, R. W. Crompton, B. C. Saha, and Z. Lj. Petrovic, Aust. J. Phys. **40**, 239 (1987).
[28]N. T. Lee and L. C. G. Freitas, J. Phys. B **14**, 4691 (1981).
[29]D. G. Truhlar and J. K. Rice, J. Chem. Phys. **52**, 4480 (1970); D. G. Truhlar, Phys. Rev. A **7**, 2217 (1973).
[30]G. P. Arrighini, F. Biondi, and C. Guidotti, Mol. Phys. **41**, 1501 (1980).
[31]G. P. Arrighini, F. Biondi, C. Guidotti, A. Biagi, and F. Marinelli, Chem. Phys. **52**, 133 (1980).
[32]M. Cacciatore and M. Capitelli, Chem. Phys. **55**, 67 (1981).
[33]S. Chung, C. C. Lin, and E. T. P. Lee, Phys. Rev. A **12**, 1340 (1975).
[34]S. Chung and C. C. Lin, Phys. Rev. A **17**, 1874 (1978).
[35]A. G. Domenicucci and K. J. Miller, J. Chem. Phys. **66**, 3827 (1977).
[36]A. W. Fliflet and V. McKoy, Phys. Rev. A **21**, 1863 (1980).
[37]A. U. Hazi, Phys. Rev. A **23**, 2232 (1981).
[38]T. K. Holley, S. Chung, C. C. Lin, and E. T. Lee, Phys. Rev. A **25**, 1852 (1982).
[39]W. Kolos, H. J. Monkhorst, and K. Szalewicz, J. Chem. Phys. **77**, 1335 (1982).
[40]M. T. Lee, R. R. Lucchese, and V. McKoy, Phys. Rev. A **26**, 3240 (1982).
[41]T. N. Rescigno, C. W. McCurdy, Jr., and V. McKoy, J. Phys. B **8**, L433 (1975); T. N. Rescigno and B. I. Schneider, J. Phys. B **21**, L691 (1988).
[42]T. N. Rescigno, C. W. McCurdy, Jr., V. McKoy, and C. F. Bender, Phys. Rev. A **13**, 216 (1976).
[43]J. C. Steelhammer and C. W. Lipsky, J. Chem. Phys. **53**, 1445 (1970).
[44]C. A. Weatherford, Phys. Rev. A **22**, 2519 (1980).
[45]M. J. Redmon, B. C. Garrett, L. T. Redmon, and C. W. McCurdy, Phys. Rev. A **32**, 3354 (1985).
[46]K. L. Baluja, C. J. Noble, and J. Tennyson, J. Phys. B **18**, L851 (1985).
[47]B. I. Schneider and L. A. Collins, J. Phys. B **18**, L857 (1985); Phys. Rev. A **33**, 2982 (1986).
[48]M. A. P. Lima, T. L. Gibson, W. M. Huo, and V. McKoy, J. Phys. B **18**, L865 (1985); M. A. P. Lima, T. L. Gibson, V. McKoy, and W. M. Huo, Phys. Rev. A **38**, 4527 (1988).
[49]G. R. Möhlmann and F. J. de Heer, Chem. Phys. **40**, 157 (1979); G. R. Mohlmann, F. J. de Heer, and J. Los, Chem. Phys. **25**, 103 (1977).
[50]D. A. Vroom and F. J. de Heer, J. Chem. Phys. **150**, 580 (1969).
[51]G. A. Khayrallah, Phys. Rev. A **13**, 1984 (1976).
[52]C. Karolis and E. Harting, J. Phys. B **11**, 357 (1971).

Downloaded 24 Jun 2013 to 128.112.200.107. This article is copyrighted as indicated in the abstract. Reuse of AIP content is subject to the terms at: http://jpcrd.aip.org/about/rights_and_permissions

[53]M. J. Mumma and E. C. Zipf, J. Chem. Phys. **55**, 1661 (1971).
[54]W. E. Kauppila, P. J. O. Tuebner, W. L. Fite, H. I. Girnius, and J. E. Giemius, J. Chem. Phys. **54**, 1670 (1971).
[55]R. L. Long, D. M. Cox, and S. J. Smith, J. Res. NBS **72A**, 521 (1968).
[56]J. D. Carriere and F. J. de Heer, J. Chem. Phys. **56**, 2993 (1972).
[57]G. R. Möhlmann, K. H. Shima, and F. J. de Heer, Chem. Phys. **28**, 331 (1978).
[58]B. van Zyl, M. W. Gealy, and H. Neumann, Phys. Rev. A **31**, 2922 (1985).
[59]J. M. Woolsey, J. L. Forand, and J. W. McConkey, J. Phys. B **19**, L495 (1986).
[60]A. McPherson, N. Rouze, W. B. Westveld, and J. S. Risley, Appl. Opt. **25**, 298 (1986).
[61]D. M. Cox and S. J. Smith, Phys. Rev. A **5**, 2428 (1972).
[62]J. A. Shiavone, S. M. Tarr, and R. S. Freund, J. Chem. Phys. **70**, 4468 (1979).
[63]B. L. Carnahan and E. C. Zipf, Phys. Rev. A **16**, 991 (1977).
[64]E. J. Stone and E. C. Zipf, J. Chem. Phys. **56**, 4646 (1972).
[65]J. M. Ajello, S. K. Srivastava, and Y. L. Yung, Phys. Rev. A **25**, 2485 (1982).
[66]H. Tawara and T. Kato, At. Data & Nucl. Data Tables **36**, 167 (1987).
[67]In IPPJ-DT-48 edited by K. Takayanagi and H. Suzuki (Institute of Plasma Physics, Nagoya University, Nagoya, 1975).
[68]A. K. Edwards, R. M. Wood, A. S. Beard, and R. L. Ezell, Phys. Rev. A **37**, 3697 (1988).
[69]G. J. Schultz and R. K. Asundi, Phys. Rev. **158**, 25 (1967).
[70]D. Rapp, J. E. Sharp, and D. D. Briglia, Phys. Rev. Letters **14**, 533 (1965).
[71]M. Allan and S. F. Wong, Phys. Rev. Letters **41**, 1791 (1978).
[72]J. M. Wadera and J. N. Bardsley, Phys. Rev. Letters **41**, 1795 (1978); Phys. Rev. A **20**, 1398 (1979); J. M. Wadera, Phys. Rev. A **29**, 106 (1984); J. P. Gauyacq, J. Phys. B **18**, 1859 (1985).
[73]C. Bottcher, J. Phys. B **9**, 2899 (1976).
[74]G. H. Dunn and B. van Zyl, Phys. Rev. **154**, 40 (1967).
[75]B. Peart and K. T. Dolder, J. Phys. B **4**, 1496 (1971).
[76]B. Peart and K. T. Dolder, J. Phys. B **5**, 1554 (1972).
[77]B. Peart and K. T. Dolder, J. Phys. B **6**, 2409 (1973).
[78]B. Peart and K. T. Dolder, J. Phys. B **8**, 1570 (1975).
[79]B. Peart and K. T. Dolder, J. Phys. B **5**, 860 (1972).
[80]D. Auerbach, R. Casak, R. Caudano, T. D. Gaily, C. J. Keyser, J. Wm. McGowan, J. B. A. Mitchell, and S. F. G. Wilk, J. Phys. B **10**, 3797 (1977).
[81]A. Guisti-Suzor, J. N. Bardsley, and C. Derkits, Phys. Rev. A **28**, 682 (1983).
[82]H. Takagi and H. Nakamura, J. Chem. Phys. **84**, 2431 (1986); K. Nakashima, H. Takagi, and H. Nakamura, J. Chem. Phys. **86**, 726 (1987).
[83]P. Hickman, J. Phys. B **20**, 2091 (1987).
[84]B. Peart and K. T. Dolder, J. Phys. B **7**, 236 (1974).
[85]D. Marthur, S. U. Khan, and J. B. Hasted, J. Phys. B **11**, 3615 (1978).
[86]H. Hus, F. Yousif, C. Noren, A. Sen, and J. B. A. Mitchell, Phys. Rev. Letters **60**, 1006 (1988).
[87]M. Voyler and G. H. Dunn, Phys. Rev. A **11**, 1983 (1975).
[88]R. A. Phaneuf, D. H. Crandall, and G. H. Dunn, Phys. Rev. A **11**, 528 (1975).
[89]B. Peart and K. T. Dolder, J. Phys. B **6**, L359 (1973).
[90]B. Peart and K. T. Dolder, J. Phys. B **7**, 1948 (1974).
[91]J. A. Macdonald, M. A. Biondi, and R. Johnsen, Planet. Space Sci. **32**, 651 (1984).
[92]M. T. Leu, M. A. Biondi, and R. Johnsen, Phys. Rev. A **8**, 413 (1973).
[93]N. G. Adams, D. Smith, and E. Alge, J. Chem. Phys. **81**, 1778 (1984); N. G. Adams and D. Smith, in *Astrochemistry*, edited by M. S. Vardya and S. P. Tarafdar (Reidel, 1987), p. 1.
[94]H. Hus, F. Yousif, A. Sen, and J. B. A. Mitchell, Phys. Rev. A **38**, 658 (1988).
[95]T. Amano, Astrophys. J. **329**, L121 (1988).
[96]J. B. A. Mitchell, C. T. Ng, L. Forand, R. Janssen, and J. Wm. McGowan, J. Phys. B **17**, L909 (1984).
[97]J. B. A. Mitchell, J. L. Forand, C. T. Ng, D. P. Levac, R. E. Mitchell, P. M. Mul, W. Claeys, A. Sen, and J. Wm. McGowan, Phys. Rev. Letters **51**, 885 (1983).
[98]B. Peart, R. A. Forrest, and K. T. Dolder, J. Phys. B **12**, 3441 (1979).
[99]B. Peart and K. T. Dolder, J. Phys. B **7**, 1567 (1974).
[100]B. Peart and K. T. Dolder, J. Phys. B **8**, L143 (1974).
[101]H. H. Michels and R. H. Hobbs, Astrophys. J **286**, L27 (1984).
[102]M. A. Khakoo, S. Trajmar, R. McAdams, and T. W. Shyn, Phys. Rev. A **35**, 2832 (1987).
[103]B. Jaduszliwer, Abstract book of XV ICPEAC (Brighton, 1987), p. 812.
[104]R. S. Freund, J. A. Shiavone, and P. F. Brader, J. Chem. Phys. **64**, 1122 (1976).
[105]M. Leventhal, R. T. Robiscoe, and K. R. Lea, Phys. Rev. **158**, 49 (1967).
[106]J. J. Spezeski, O. F. Kalman, and L. C. McIntyre, Jr., Phys. Rev. A **22**, 1906 (1980); S. R. Ryan, J. J. Spezeski, O. F. Kalman, O. F. Lamb, and H. H. Wing, Phys. Rev. A **19**, 2192 (1979).
[107]M. Misakian and J. C. Zorn, Phys. Rev. A **6**, 2180 (1972).
[108]H. Cho, K. C. Hsien, and L. C. McIntyre, Jr., Phys. Rev. A **33**, 2290 (1986).
[109]N. Bose, J. Phys. B **11**, L309 (1978).
[110]K. Ito, N. Oda, Y. Hatano, and T. Tsuboi, Chem. Phys. **21**, 203 (1977).
[111]L. D. Weaver and R. H. Hughes, J. Chem. Phys. **52**, 2299 (1979).
[112]T. Ogawa and M. Higo, Chem. Phys. **52**, 243 (1982); J. Kurawaki and T. Ogawa, Chem. Phys. **86**, 296 (1984).
[113]M. Higo, S. Kamata, and T. Ogawa, Chem. Phys. **66**, 243 (1982).
[114]N. Takahashi, S. Arai, N. Kouchi, N. Oda, and Y. Hatano, J. Phys. B **16**, 1547 (1983); K. Nakashima, H. Tomura, and T. Ogawa, Chem. Phys. **138**, 138 (1987).
[115]G. H. Dunn and L. J. Kieffer, Phys. Rev. **132**, 2109 (1963).
[116]A. Crowe and J. W. McConkey, J. Phys. B **6**, 2088 (1973).
[117]P. Rapp, P. Englander-Golden and P. B. Briglia, J. Chem. Phys. **42**, 4081 (1965).
[118]G. H. Dunn, Phys. Rev. Letters **8**, 62 (1962).
[119]A. Crowe and J. W. McConkey, Phys. Rev. Letters **31**, 192 (1973); J. A. Stockdale, V. E. Anderson, A. E. Carter, and L. Deleanu, J. Chem. Phys. **63**, 3886 (1975).
[120]K. Kallmann, J. Phys. B **11**, 339 (1978).
[121]M. A. Khakoo and S. K. Srivastava, J. Phys. B **18**, 2525 (1985).
[122]N. Zare, J. Chem. Phys. **47**, 204 (1967).
[123]R. J. van Brunt and L. J. Kieffer, Phys. Rev. A **2**, 1293 (1970).
[124]K. E. McCulloh and H. M. Rosenstock, J. Chem. Phys. **48**, 2084 (1968).
[125]H. Tawara, Y. Itikawa, Y. Itoh, T. Kato, H. Nishimura, S. Ohtani, H. Takagi, K. Takayanagi, and M. Yoshino, IPPJ-AM-46 (Institute of Plasma Physics, Nagoya University, Nagoya 464-01) (1986).
[126]H. Tawara, Y. Itikawa, H. Nishimura, and M. Yoshino, IPPJ-AM-55 (Institute of Plasma Physics, Nagoya University, Nagoya 464-01) (1987).
[127]C. B. Opal, E. C. Beaty, and W. K. Peterson, At. Data Tables **4**, 209 (1972).
[128]M. Inokuti, Rev. Mod. Phys. **43**, 297 (1971); M. Inokuti, Y. Itikawa, and J. R. Turner, Rev. Mod. Phys. **50**, 23 (1978).

Downloaded 24 Jun 2013 to 128.112.200.107. This article is copyrighted as indicated in the abstract. Reuse of AIP content is subject to the terms at: http://jpcrd.aip.org/about/rights_and_permissions